AEC RESEARCH AND DEVELOPMENT REPORT

ORNL-2113
C-84—Reactors-Special

cy. 4-A

Features of Aircraft Reactors

BASIC GAMMA-RAY DATA FOR ART HEAT DEPOSITION CALCULATIONS

H. W. Bertini
C. M. Copenhaver
A. M. Perry
R. B. Stevenson

OAK RIDGE NATIONAL LABORATORY
OPERATED BY
UNION CARBIDE NUCLEAR COMPANY
A Division of Union Carbide and Carbon Corporation
UCC
POST OFFICE BOX P · OAK RIDGE, TENNESSEE

ORNL-2113
C-84 - Reactors-Special Features of Aircraft Reactors

This document consists of 76 pages.
Copy 4 of 264 copies. Series A.

Contract No. W-7405-eng-26

AIRCRAFT REACTOR ENGINEERING DIVISION

BASIC GAMMA-RAY DATA FOR ART HEAT DEPOSITION CALCULATIONS

H. W. Bertini
C. M. Copenhaver
A. M. Perry
R. B. Stevenson

DATE ISSUED

SEP 17 1956

OAK RIDGE NATIONAL LABORATORY
Operated by
UNION CARBIDE NUCLEAR COMPANY
A Division of Union Carbide and Carbon Corporation
Post Office Box P
Oak Ridge, Tennessee

ORNL-2113
C-84 - Reactors-Special Features
of Aircraft Reactors

INTERNAL DISTRIBUTION

1. C. E. Center
2. Biology Library
3. Health Physics Library
4-5. Central Research Library
6. Reactor Experimental Engineering Library
7-11. Laboratory Records Department
12. Laboratory Records, ORNL R.C.
13. A. M. Weinberg
14. L. B. Emlet (K-25)
15. J. P. Murray (Y-12)
16. J. A. Swartout
17. E. H. Taylor
18. E. D. Shipley
19. M. L. Nelson
20. G. H. Clewett
21. S. C. Lind
22. F. L. Culler
23. L. G. Alexander
24. L. B. Anderson
25. S. J. Cromer
26. P. R. Bell
27. H. W. Bertini
28. E. S. Bettis
29. E. P. Blizard
30. A. L. Boch
31. A. D. Callihan
32. R. A. Charpie
33. H. C. Claiborne
34. T. E. Cole
35. C. M. Copenhaver
36. W. B. Cottrell
37. S. J. Cromer
38. L. Dresner
39. C. E. Winters
40. W. K. Ergen
41. A. P. Fraas
42. H. W. Hoffman
43. W. H. Jordan
44. P. R. Kasten
45. G. W. Keilholtz
46. W. E. Kinney
47. M. E. LaVerne
48. D. D. Cowen
49. J. A. [illegible]
50. R. S. Livingston
51. F. C. [illegible]
52. W. D. [illegible]
53. R. V. [illegible]
54. H. Moran
55. A. M. Perry
56. R. W. Peelle
57. D. E. Plaus
58. D. L. Plaus
59. H. F. Poppendiek
60. M. W. Rosenthal
61. M. T. Robinson
62. H. W. Savage
63. Dunlap Scott, Jr.
64. A. Simon
65. R. [illegible] Stevenson
66. D. [illegible]
67. D. K. Trubey
68. C. D. Zerby
69. J. H. Frye, Jr.
70-71. ORNL - Y-12 Technical Library, Document Reference Section

EXTERNAL DISTRIBUTION

72. AF Plant Representative, Baltimore
73. AF Plant Representative, Burbank
74. AF Plant Representative, Marietta
75. AF Plant Representative, Santa Monica
76. AF Plant Representative, Seattle
77. AF Plant Representative, Wood-Ridge
78. Air Materiel Area
79. Air Research and Development Command (RDGN)
80. Air Research and Development Command (RDZPA)
81. Air Technical Intelligence Center

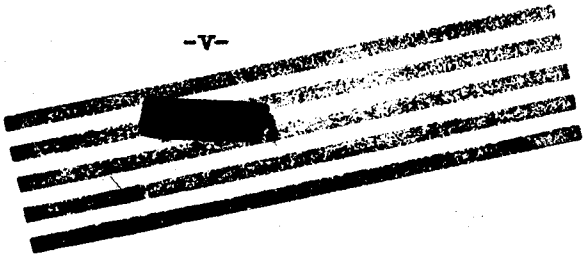

TABLE OF CONTENTS

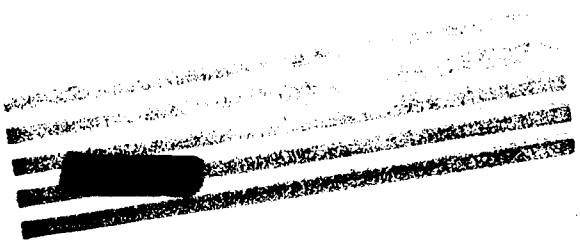

LIST OF ILLUSTRATIONS

LIST OF TABLES

The data in this report are based on references dated up to March 30, 1956. However, recently available experimental information* appears to be in good agreement with this data.

* R. M. Sinclair, Phys. Rev. 102, 461 (1956).
R. B. Day, Phys. Rev. 102, 767 (1956).
T. H. Braid, Phys. Rev. 102, 1109 (1956).

[redacted]

INTRODUCTION

In order that fairly accurate thermal stress calculations can be made on the ART, it is necessary to have a reasonable picture of the temperature distribution in the reactor. To get the temperature distributions, and to determine cooling requirements in various parts of the reactor, one must know the heat deposition rates due to alpha particles, beta rays, gamma rays, and neutrons in all parts of the reactor.

The present report contains only the basic physical data necessary to determine the heat deposition rates due to gamma rays.

Neutron fluxes in the core and reflector regions of the ART are to be obtained from two-dimensional multigroup calculations (performed by the Curtiss-Wright Corporation). These fluxes, in conjunction with the neutron absorption cross sections, determine the neutron capture and inelastic scattering rates in the core and in the reflector. The data in this report permit the calculation of the number of gamma rays originating at various energies at every point in the core and reflector.

The data are presented in the form of the number of photons at particular energies per event. The photon energy groups were chosen to correspond to the energies at which it was most convenient to calculate the energy absorption buildup factors.

A considerable amount of work on the gamma rays resulting from inelastically scattered neutrons is included here in some detail, in order to clarify the reasons for using the values tabulated here for this reaction. It is recognized that the treatment of the subject given here is not exhaustive, and may be subject to revision when further experimental or theoretical information is available.

The multigroup intervals used by the Curtiss-Wright Corporation in their calculations of the neutron fluxes in the ART are given (Table 8).

[redacted]

[redacted]

PROMPT GAMMA RAYS AND U^{235} CAPTURE GAMMA RAYS IN THE FUEL

Prompt Gamma Rays

The prompt gamma-ray information included here was obtained from the Ph.D. dissertation of Roger Gamble.[1] The prompt gamma-ray spectrum can be approximated by

$$N'(E) = 7.6\ e^{-1.01E} \text{ photons/(Mev)(fission)}.$$

The expression

$$\frac{N'(E)}{10} = 0.76\ e^{-1.01E} \text{ (photons/(100 kev)(fission)},$$

is superimposed on the results of Gamble's work in Fig. 1 to illustrate the fit of the curve with the experimental data.

The total number of photons and total energy released per fission can be obtained as follows:

$$N_T' = \int_0^\infty N'(E)\ dE = 7.52 \text{ photons/fission},$$

$$E_T' = \int_0^\infty E\ N'(E)\ dE = 7.45 \text{ Mev/fission}.$$

These values agree with the respective values obtained by Gamble ($N_T' = 7.51$; $E_T' = 7.46$) using the measured spectra.

Capture Gamma Rays in U^{235}

Apparently there are no data available on the spectrum of gamma rays resulting from radiative neutron capture in U^{235}. The resulting capture gamma rays will probably be of spectral type 3, as indicated by a study of the spectral types of other heavy elements. Mittleman[2] defines type 3

---

1. R. L. Gamble, Prompt Fission Gamma Rays from Uranium 235, unpublished dissertation done at Oak Ridge National Laboratory (June, 1955).
2. P. S. Mittleman, and R. A. Liedtke, "Gamma Rays from Thermal-Neutron Capture", Nucleonics, Vol. 13, No. 5, 50 (1955).

[redacted]

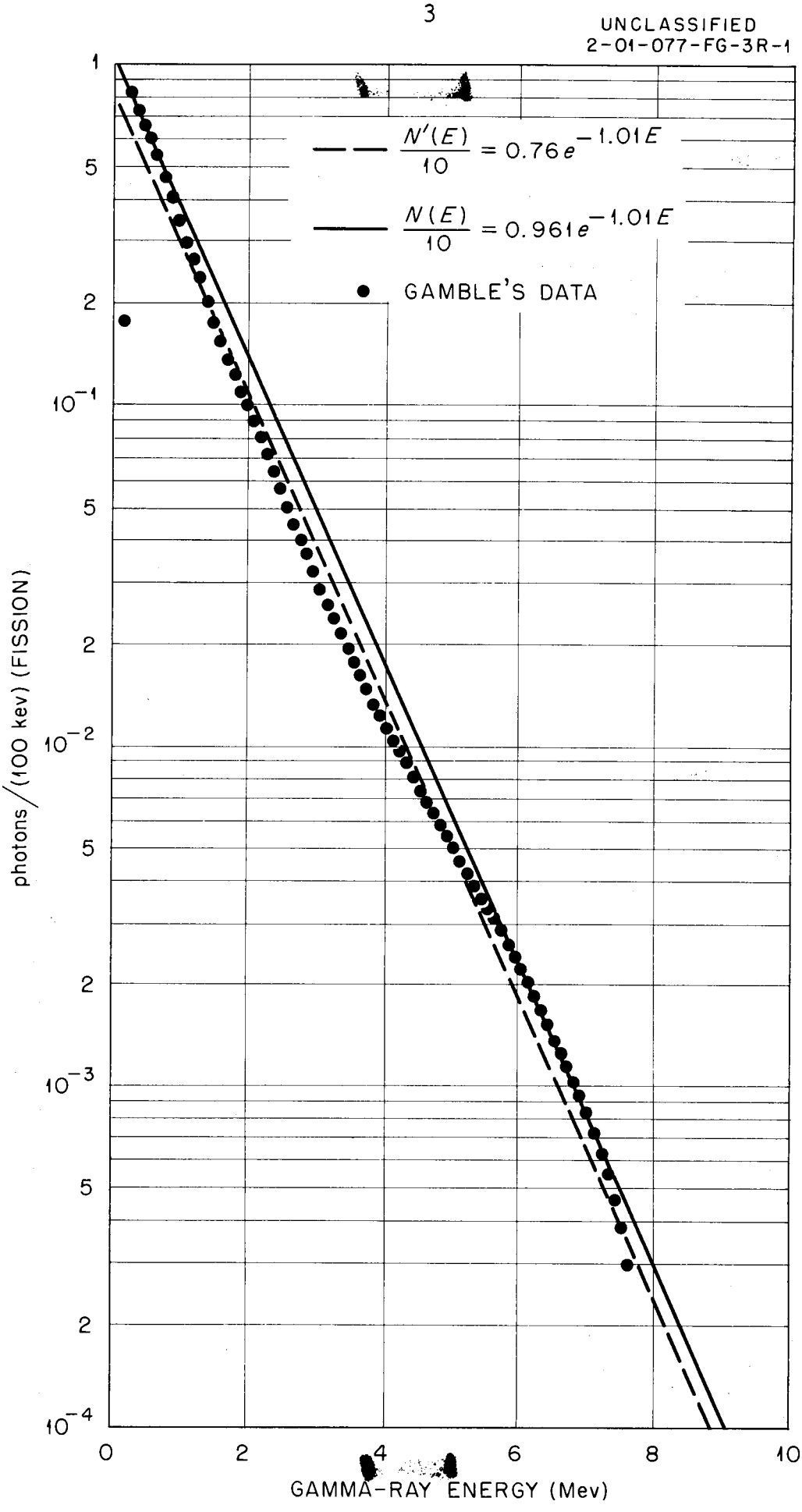

Fig. 1. Prompt Gamma Spectrum of U^{235}.

[redacted]

capture gamma-ray spectra as having many gamma rays, no line structure below 5 Mev, and with the distribution peaking below one-half maximum energy.

For a reactor operating essentially on thermal neutrons the total energy of the U^{235} capture gammas released per fission can be obtained from

$$E_T = \frac{\sigma_c^{th}(U^{235})}{\sigma_f^{th}(U^{235})} \times \text{(binding energy of additional neutrons in } U^{235}),$$

where

σ_c^{th} ≡ thermal absorption cross section minus thermal fission cross section.

Therefore

$$E_T = \frac{107 \text{ barns}}{580 \text{ barns}} \times 6.426 \text{ Mev}^3 = 1.18 \text{ Mev/fission}$$

for a thermal reactor. (The cross section values were taken from the work of Hughes and Harvey.[4])

In the ART, approximately 40% of the fissions are due to thermal neutrons and 60% are due to epithermal neutrons,[5] so the variation of α, i.e., σ_c/σ_f, with energy must be taken into account. This was done by calculating the ratio of the total number of U^{235} captures in the core of the ART to the total number of fissions. The data used in this calculation were taken from the output of multigroup calculations performed by the Curtiss-Wright Corporation on a spherical model of the ART.[5] The cross sections used were Curtiss-Wright multigroup cross sections.[6] For the calculation,

---

3. The Reactor Handbook, Vol. 1, Physics.
4. D. J. Hughes and J. A. Harvey, Neutron Cross Sections, BNL 325 (July 1, 1955).
5. H. Reese, Jr., S. Strauch and J. Mihalczo, Geometry Study for an ANP Circulating Fuel Reactor, WAD-1901, Fig. 134 (Sept. 1, 1954).
6. D. L. Kavanagh and C. B. Mills, Neutron Cross Sections for Multigroup Reactor Calculations, CWR 413 (Sept. 1, 1955).

[redacted]

[redacted]

$$\frac{\text{number of } U^{235} \text{ captures}}{\text{number of fissions}} = \frac{\sum_i A_i \frac{\sigma_{c_i}}{\sigma_{a_i}}}{\sum_i F_i} \times 0.98$$

$$= 0.306 \text{ captures/fission in } U^{235},$$

where

$A_i \equiv$ number of absorptions in the fuel region in the i^{th} lethargy group,

$F_i \equiv$ number of fissions in the fuel region in the i^{th} lethargy group,

$\sigma_{c_i} \equiv$ average capture cross section of U^{235} in i^{th} lethargy group,

$\sigma_{a_i} \equiv$ average absorption cross section of U^{235} in the i^{th} lethargy group.

The factor 0.98 arises from the fact that 98% of the absorptions in the fuel region are absorptions in U^{235}. For the ART,

$$E''_T = 0.306 \frac{\text{capture}}{\text{fission}} \times 6.426 \frac{\text{Mev}}{\text{capture}} = 1.97 \frac{\text{Mev}}{\text{fission}} \text{ in } U^{235}.$$

Since the total energy E''_T is small relative to that of the prompt gamma rays and probably of spectral type 3, the U^{235} capture gamma-ray spectrum was assumed to have the same spectral distribution as that of the prompt gamma rays. Thus, for the ART

$$N''(E) = 2.01\, e^{-1.01E} \text{ photons/(Mev)(fission)}.$$

Prompt Gamma Rays Plus U^{235} Capture Gamma Rays

The spectrum of prompt gamma rays plus the U^{235} capture gamma rays is, by addition,

$$N(E) = 9.61\, e^{-1.01E} \text{ photons/(Mev)(fission)}.$$

A plot of $0.961\, e^{-1.01E}$ photons/(100 kev)(fission) is shown in Fig. 1. Tabulations of the pertinent information are presented in Tables 1 and 2, and the equations used are presented in the following summary.

[redacted]

[redacted]

Spectrum:

$$N(E) \equiv \text{number of photons/(Mev)(fission)}$$

For prompt plus U^{235} capture gamma rays

$$N(E) = 9.61\, e^{-1.01E} \text{ photons/(Mev)(fission)}$$

Total number of photons per fission:

$$N_T = \int_o^\infty N(E)\, dE = 9.51 \text{ photons/fission}$$

Total energy per fission:

$$E_T = \int_o^\infty E\, N(E)\, dE = 9.42 \text{ Mev/fission}$$

Average energy per photon:

$$\overline{E}_\gamma = \frac{\int_o^\infty E\, N(E)\, dE}{\int_o^\infty N(E)\, dE} = 0.99 \text{ Mev/photon}$$

Average power density in the core:

$$3.21 \text{ ft}^3 \text{ of fuel volume in the core}^7 = 9.09 \times 10^4 \text{ cm}^3$$

$$(9.42 \text{ Mev/fission} \times 3.1 \times 10^{10} \text{ fission/sec·watt} \times$$

$$6 \times 10^7 \text{ watt} \times 1.6 \times 10^{-13} \text{ watt·sec/Mev})/9.09 \times 10^4 \text{ cm}^3$$

$$= 30.9 \text{ watts/cm}^3 \text{ of fuel in core.}$$

---

7. W. L. Scott, Jr., Dimensional Data for the ART, ART Design Data Sheet No. 8-A-3, p 10 (Jan. 27, 1956).

[redacted]

[redacted]

Table 1. Prompt and U^{235} Capture Gamma Rays, Energy Per Fission in Various Energy Intervals

$$E_{ab} = \int_a^b E\, N(E)\, dE$$

a (Mev)	b (Mev)	E_{ab} (Mev/fission)
0	0.75	1.655
0.75	1.5	2.553
1.5	3.0	3.374
3.0	5.0	1.472
5.0	7.0	0.3012
7.0	9.0	0.0539
9.0	11.0	0.00904
	Total =	9.42 Mev/fission

[redacted]

[redacted]

Table 2. Prompt and U^{235} Capture Gamma Rays, Photons Per Fission in Various Energy Intervals

(Photons/fission at $\overline{E}$) x $\overline{E}$ = E_{ab}

a (Mev)	b (Mev)	$\overline{E}$ (Mev)	Photons/fission at $\overline{E}$
0	0.75	0.5	3.31
0.75	1.5	1.0	2.55
1.5	3.0	2.0	1.687
3.0	5.0	4.0	0.3680
5.0	7.0	6.0	0.0502
7.0	9.0	8.0	0.00674
9.0	11.0	10.0	0.000904

$\overline{E}$ chosen to correspond to energies at which buildup factors were calculated.

[redacted]

[redacted]

DECAY GAMMA RAYS IN THE FUEL

The fission-fragment-decay gamma-ray spectrum was obtained principally from experiments of Peelle, Zobel, and Love,[8] who used a multiple-crystal gamma-ray spectrometer and a circulating fuel belt with transit times between 1.2 and 2.5 sec. The measured gamma-ray spectrum can be approximated by

$$N_1(E) = 9.0\, e^{-1.33E} \text{ photons/(Mev)(fission)}.$$

In Fig. 2 the curve of $N_1(E)$ vs E is superimposed on the curve experimentally determined by Peelle et al. for comparison purposes. Integration of this spectrum between 0.36 and 5.8 Mev results in 4.2 photons/fission and 4.7 Mev/fission, which agree quite well with values (4.2 photons/fission, 4.8 Mev/fission) obtained by integration of the measured spectrum.[8]

The time of irradiation, T, of the circulating fuel belt was 10^4 sec ($\sim$3 hr), and the fraction of the saturation activity of the long-lived nuclides measured is $1 - e^{-\lambda_i T}$, where λ_i is the decay constant of the i^{th} nuclide. The use of saturation activity is valid since 500 hr of full power operation of the ART would result in 96% saturation of the fission-product-decay gamma-ray energy, as indicated by Moteff.[9] The increase in the decay gamma-ray spectrum due to the long-lived fission fragments was obtained by multiplying the photons per fission for each nuclide, given in a compilation by Blomeke,[10] by the fraction of the saturation activity not measured, and adding to the measured gamma-ray spectrum given previously. Blomeke's compilation was used in preference to similar compilations by Moteff[9] and Clark[11] because of the larger list of nuclides included. Blomeke's list includes nuclides having very small yields (10^{-5} % and above), nuclides which emit gamma rays with energies down to 0.01 Mev, and nuclides with short half lives ($\sim$1 sec and greater).

---

8. R. W. Peelle, T. A. Love and W. Zobel, ANP Quar. Prog. Rep. Dec. 10, 1955, ORNL-2012, Part I, II, III, p 223-226.
9. J. Moteff, Fission Product Decay Gamma Energy Spectrum, APEX-134 (1953).
10. J. O. Blomeke, Nuclear Properties of U-235 Fission Products, ORNL CF-54-12-52 (1954).
11. F. H. Clark, Decay of Fission Product Gammas, NDA-27-39 (1955).

[redacted]

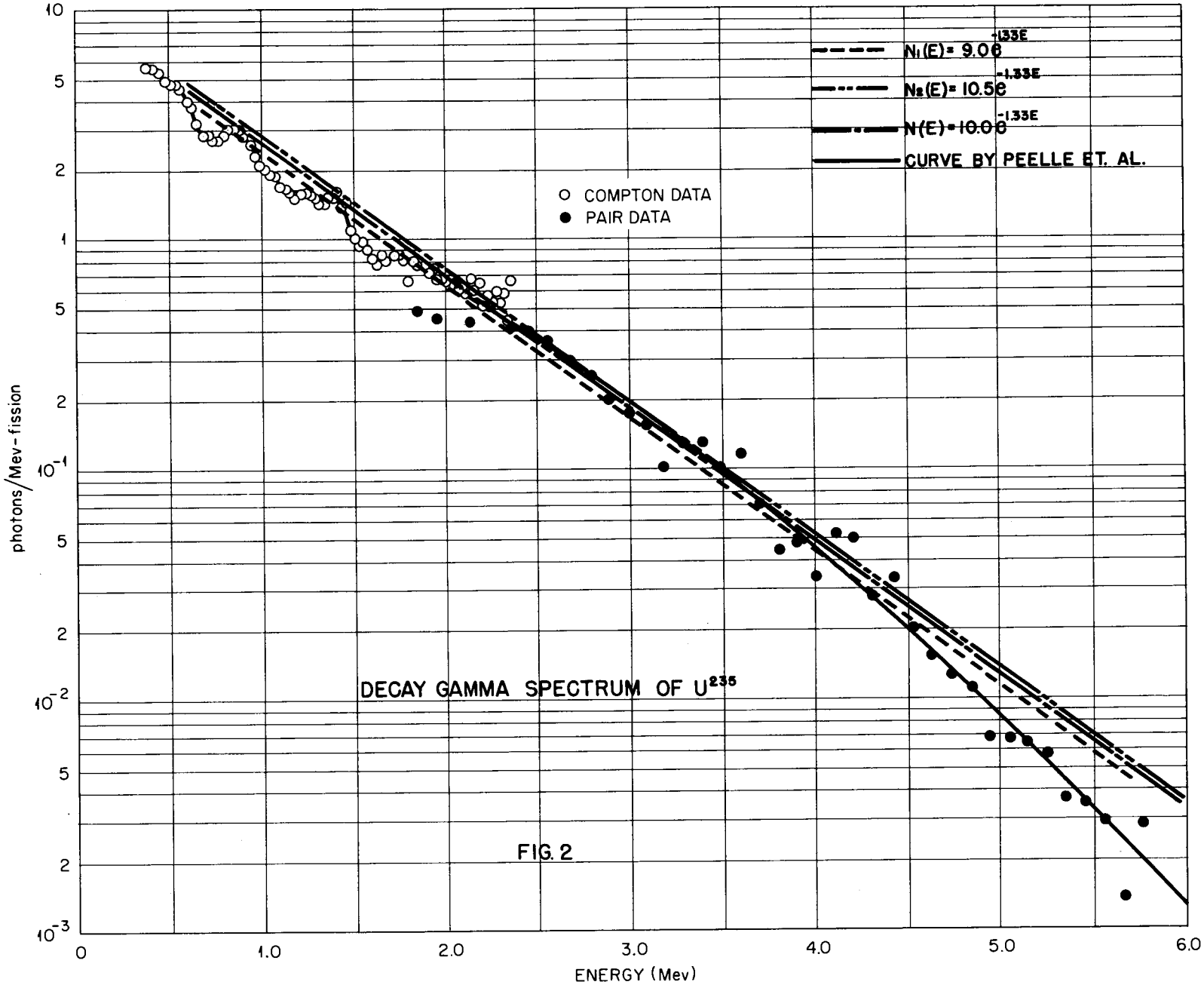
$N_1(E) = 9.0e^{-1.33E}$
$N_2(E) = 10.5e^{-1.33E}$
$N(E) = 10.0e^{-1.33E}$
CURVE BY PEELLE ET. AL.
COMPTON DATA
PAIR DATA
DECAY GAMMA SPECTRUM OF U^{235}
photons/Mev-fission
ENERGY (Mev)
10
5
2
1
5
2
10^{-1}
5
2
10^{-2}
5
2
10^{-3}
0
1.0
2.0
3.0
4.0
5.0
6.0

FIG. 2

[redacted]

For nuclides having a half life of 1/3 sec, which partially decay between activation and detection, 85% of the saturation activity was estimated to have been measured.[12] There is experimental evidence[13] that there are no fission products with half lives less than about 0.5 sec. This is in accord with beta-ray theory, which predicts that the excitation energy for middle weight nuclides would have to be greater than the neutron binding energy for the half life to be shorter than 0.5 sec. Also, the short-lived nuclides will not affect the decay gamma-ray source strength for fuel outside the core of the ART. Since the transit time of the fuel is about 3 sec, most fission-product nuclides are assumed to be uniformly distributed throughout the fuel volume. The resulting gamma-ray spectrum, without considering purging of the fission-product gases from the fuel, can be approximated by

$$N_2(E) = 10.5\, e^{-1.33E} \text{ photons/(Mev)(fission)}.$$

This curve is illustrated in Fig. 2. Even though an estimated probable error of ± 20% is assigned to this spectrum, it is interesting to note that the total energy released per fission is 5.9 Mev and that Way[14] estimated, on theoretical grounds, a total of approximately 6 Mev/fission.

From a knowledge of the saturation activities of the xenon and krypton gaseous fission products with purging and without purging,[15] a simple ratio can be obtained as follows:

$$F \equiv \frac{\text{saturation activity with purging}}{\text{saturation activity without purging}} = \frac{\lambda_i + \sigma_i \phi_o}{\lambda_p + \lambda_i + \sigma_i \phi_o},$$

where

λ_i = the decay constant of the i^{th} nuclide,

σ_i = the absorption cross section of the i^{th} nuclide,

---

12. R. W. Peelle, private communication.
13. J. E. Brolley, D. H. Cooper, W. S. Hall, M. S. Livingston and L. K. Schlacks, Phys. Rev. 83, 990 (Sept. 1, 1951).
14. K. Way, Mon P-192 (1946).
15. J. L. Meem, The Xenon Problem in the ART, ORNL CF-54-5-1 (May 3, 1954).

[redacted]

[redacted]

ϕ_o = the neutron flux

λ_p = purging constant = 8.3×10^{-3} sec^{-1} .[15]

With the exception of Xe^{135}, $\sigma_i \phi_o$ will be negligible and the ratio will reduce to

$$F = \frac{\lambda_i}{\lambda_p + \lambda_i} .$$

The decrease in the decay gamma-ray spectrum due to purging was readily found by using the above ratio and the saturation activities of the gamma-emitting xenons, kryptons and the daughters of xenon and krypton.[10] The final resulting decay gamma-ray spectrum at steady state can be approximated by

$$N(E) = 10.0\ e^{-1.33E} \text{ photons/(Mev)(fission)} ,$$

which is illustrated in Fig. 2.

The long-lived fission fragments increased the total energy per fission of the measured spectrum by about 17%, and the decrease in the total energy per fission due to purging is approximately 5%. A summary of the pertinent decay gamma-ray information is given in the following equations and Tables 3 and 4.

[redacted]

[redacted]

Spectrum:

$$N(E) \equiv \text{number of photons/(Mev)(fission)}$$

$$N(E) = 10\, e^{-1.33E} \text{ photons/(Mev)(fission)}$$

Total number of photons per fission:

$$N_T = \int_0^\infty N(E)\, dE = 7.52 \text{ photons/fission}$$

Total number of photons per fission per unit volume of fuel:

$$N_T/V = 7.52/2.45 \times 10^{5*} = 3.07 \times 10^{-5} \text{ photons/(fission)(cm}^3\text{)}$$

Total energy per fission:

$$E_T = \int_0^\infty E\, N(E)\, dE = 5.65 \text{ Mev/fission}$$

Total energy per fission per unit volume of fuel:

$$\frac{5.65}{2.45 \times 10^5} = 2.31 \times 10^{-5} \text{ Mev/(fission)(cm}^3\text{)}$$

Average energy per photon:

$$\bar{E}_\gamma = \frac{\int_0^\infty E\, N(E)\, dE}{\int_0^\infty N(E)\, dE} = 0.75 \text{ Mev/photon}$$

Average energy per photon per unit volume of fuel:

$$\frac{0.75}{2.45 \times 10^5} = 3.06 \times 10^{-6} \text{ Mev/(photon)(cm}^3\text{)}$$

---

* J. Foster, Oak Ridge National Laboratory, private communication.

[redacted]

[redacted]

Photons per second per unit volume of fuel:

$$(6 \times 10^7 \text{ watts} \times 3.1 \times 10^{10} \text{ fission/sec.watt} \times 7.52 \text{ photon/fission})/2.45 \times 10^5 \text{ cm}^3$$

$$= 5.7 \times 10^{13} \text{ photons/sec/cm}^3$$

Power density in the fuel:

$$5.7 \times 10^{13} \text{ photons/sec.cm}^3 \times 0.75 \text{ Mev/photon} \times 1.6 \times 10^{-13} \text{ watt.sec/Mev}$$

$$= 6.84 \text{ watts/cm}^3 \text{ of fuel}$$

Power density in the heat exchanger:

$$6.84 \text{ watt/cm}^3 \times 0.335 = 2.3 \text{ watt/cm}^3 \text{ of heat exchanger}$$

$$0.335 = \frac{\text{volume of fuel in heat exchanger}}{\text{volume of heat exchanger}}$$[16]

16. Calculated from ART Design Memo No. 8-J-3, Rev. 1 (Dec. 2, 1955).

[redacted]

[redacted]

Table 3. Decay Gamma Rays, Energy Per Fission in Various Energy Intervals

$$E_{ab} = \int_a^b E\, N(E)\, dE$$

a (Mev)	b (Mev)	E_{ab} (Mev/fission)	E_{ab}/cm^3 of Fuel Volume (Mev/fission·cm^3)
0	0.75	1.486	6.07×10^{-6}
0.75	1.5	1.864	7.61×10^{-6}
1.5	3.0	1.781	7.27×10^{-6}
3.0	5.0	0.466	1.98×10^{-6}
5.0	7.0	0.0505	2.06×10^{-7}
7.0	9.0	0.00484	1.98×10^{-8}
9.0	11.0	0.000426	1.74×10^{-9}

Total = 5.65 Mev/fission

[redacted]

[redacted]

Table 4. Decay Gamma Rays, Photons Per Fission in Various Energy Intervals

(Photons/fission at $\bar{E}$) x $\bar{E}$ $\cong$ E_{ab}

a (Mev)	b (Mev)	$\bar{E}$ (Mev)	Photons/fission at $\bar{E}$	Photons/fission/cm^3 of Fuel Volume
0	0.75	0.5	2.972	1.213×10^{-5}
0.75	1.5	1.0	1.864	7.61×10^{-6}
1.5	3.0	2.0	0.891	3.64×10^{-6}
3.0	5.0	4.0	0.1165	4.76×10^{-7}
5.0	7.0	6.0	0.00841	3.43×10^{-8}
7.0	9.0	8.0	0.000605	2.47×10^{-9}
9.0	11.0	10.0	0.0000426	1.74×10^{-10}

$\bar{E}$ chosen to correspond to energies at which buildup factors were calculated.

[redacted]

[redacted]

CAPTURE GAMMA RAYS

Data for capture gamma rays have been compiled for sodium, beryllium, copper, Inconel, NaK, iron, B^{10}, chromium, and nickel for several energy groups. The data are presented (in Tables 5 and 6) in the same way as that for the prompt and decay gammas, i.e.,

$$E_{ab} = \int_a^b E\, N(E)\, dE ,$$

where N(E) ≡ the number of photons per unit energy per capture.

The numbers of photons per unit energy per 100 captures (100 N(E))in the interval from 3 Mev to maximum energy were obtained from a series of papers by Bartholomew, Kinsey, and Walker.[17-21] No attempt was made to approximate the spectrum by an analytic function, as was done in the two previous cases. However, a graph of E N(E) as a function of the energy E was plotted for energies greater than about 3 Mev. The area under the curve, found by graphical integration, is proportional to the energy emitted above 3 Mev.[22] Since practically no information is available on the spectra of the low-energy capture gammas (0 to 3 Mev), just enough area was added in this region for the total area from zero to the maximum energy to account for the total binding energy of the additional neutron. It was added in such a way that the energy range from 1 to 2 Mev was responsible for slightly more energy than either of the 0- to 1-Mev or 2- to 3-Mev ranges. There is no physical reason for doing this. However, it is felt that the gamma-ray heating is quite insensitive to the particular distribution chosen for gamma rays of these low energies as long as there is an appreciable number of gamma rays of higher energy. In most cases used here, a large percentage of the total energy available is emitted by gamma rays with energies in excess

---

17. Bartholomew, Kinsey and Walker, Phys. Rev. 83, 519 (1951).
18. Bartholomew and Kinsey, Can. J. of Phys. 31, 49 (1953).
19. Bartholomew and Kinsey, Phys. Rev. 89, 386 (1953).
20. Bartholomew and Kinsey, Phys. Rev. 89, 375 (1953).
21. Bartholomew and Kinsey, Phys. Rev. 85, 1012 (1952), and Ref. 2.
22. Bartholomew and Kinsey, Can. J. of Phys. 31, 537 (1953).

[redacted]

[redacted]

Table 5. Capture Gamma Rays, Energy Per Capture in Various Energy Intervals

$$E_{ab} = \int_a^b E\, N(E)\, dE$$

a (Mev)	b (Mev)	E_{ab} (Mev/capture)[a]								
		Na	Be	Cu	Inconel	NaK	Fe	B^{10}	Cr	Ni
0	0.75	0.37	0	0.32	0.03	0.17	0.15	0.445	0.125	0
0.75	1.5	0.75	0	0.60	0.27	0.59	0.53	0	1.26	0.09
1.5	3.0	1.70	0	1.36	0.42	2.58	0.96	0	1.12	0.26
3.0	5.0	2.44	1.72	1.08	0.60	2.20	0.92	0	0.32	0.60
5.0	7.0	1.74	5.10	1.26	1.50	1.44	1.20	0	0.96	1.62
7.0	9.0	0	0	3.04	5.36	0.32	3.60	0	4.56	5.60
9.0	11.0	0	0	0	0.30	0	0.30	0	0.80	0.20
Total[b]		7.00	6.82	7.66	8.48	7.30	7.66	0.445[c]	9.145	8.37
Binding Energy		6.96[d]	6.81[e]	7.66[f]	8.45[g]	7.3[h]	7.69[g]		9.15[g]	8.40[g]

[a] The indicated references for these elements and many more for other elements are given in Ref. 2.

[b] Discrepancies between total energies and binding energies are due to round off errors in E_{ab}.

[c] F. Ajzenberg and T. Lauritsen, Rev. Modern Phys. 24, 321 (1952).

[d] Bartholomew, Kinsey and Walker, Phys. Rev. 83, 519 (1951).

[e] Bartholomew and Kinsey, Can. J. of Phys. 31, 49 (1953).

[f] Bartholomew and Kinsey, Phys. Rev. 89, 386 (1953).

[g] Bartholomew and Kinsey, Phys. Rev. 89, 375 (1953).

[h] Bartholomew and Kinsey, Phys. Rev. 85, 1012 (1952), and Ref. 2.

[redacted]

[redacted]

Table 6. Capture Gamma Rays, Photons Per Capture in Various Energy Intervals

$$(\text{Photons/capture at } \bar{E}) \times \bar{E} = E_{ab}$$

a (Mev)	b (Mev)	$\bar{E}$ (Mev)	Photons/capture at $\bar{E}$								
			Na	Be	Cu	Inconel	NaK	Fe	B^{10}	Cr	Ni
0	0.75	0.5	0.74	0	0.64	0.06	0.34	0.30	0.89	0.25	0
0.75	1.5	1.0	0.75	0	0.60	0.27	0.59	0.53	0	1.26	0.09
1.5	3.0	2.0	0.85	0	0.68	0.21	1.29	0.48	0	0.56	0.13
3.0	5.0	4.0	0.61	0.43	0.27	0.15	0.55	0.23	0	0.08	0.15
5.0	7.0	6.0	0.29	0.85	0.21	0.25	0.24	0.20	0	0.16	0.27
7.0	9.0	8.0	0	0	0.38	0.67	0.04	0.45	0	0.57	0.70
9.0	11.0	10.0	0	0	0	0.03	0	0.03	0	0.08	0.02

[redacted]

[redacted]

of 3 Mev, and the distribution above this energy is fairly well known. Thus, the error in the gamma-ray heating introduced by this arbitrary assignment of energy in the low energy region should be quite small. Graphs of E N(E) as a function of energy are shown in Figs. 3a through 3e. The solid lines represent values taken from the work of Bartholomew et al., while the dashed lines represent the extrapolation needed to account for the binding energy of the additional neutron.

The total energy for each energy interval, obtained by graphically integrating the curve of E N(E) vs E over the interval, was then divided by the average energy chosen for that interval to obtain the number of photons per capture for that particular energy. The energy intervals and the average energy chosen for each interval are the same as those chosen for the prompt and decay gamma rays.

Since no graphs of N(E) vs E were available for sodium, values for the number of photons per capture were determined from data given by Bartholomew et al.,[17] Braid,[23] and Motz.[24]

The capture gamma-ray data for compound materials, such as Inconel, were taken as the weighted sum of the data for each element in the material. The weighting factor used was the ratio of the macroscopic thermal absorption cross section of the element, in the material, to the total thermal absorption cross section of the material. Thermal cross sections were obtained from the compilation of Hughes and Harvey.[4]

A similar weighting factor was used in calculating the binding energies of the elements made up of a number of isotopes. In this case the cross section data and isotopic binding energies were taken from the listed papers by Bartholomew and Kinsey.[17-22] The cross sections from these papers are consistent with those from the report of Hughes and Harvey.[4]

---

23. J. T. Braid, Phys. Rev. 90, 355A (1953).
24. H. T. Motz, Phys. Rev. 90, 355A (1953).

[redacted]

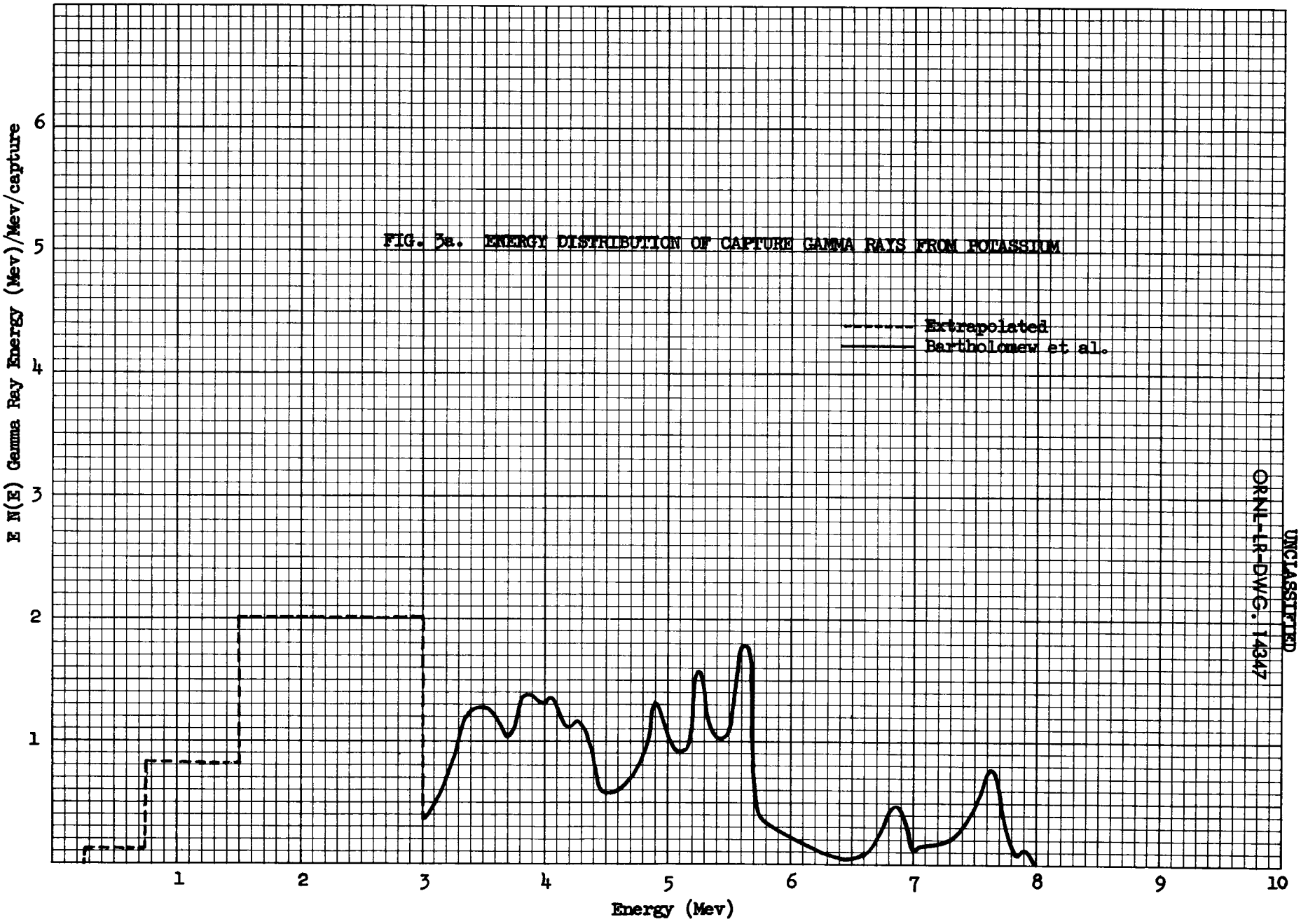

FIG. 3a. ENERGY DISTRIBUTION OF CAPTURE GAMMA RAYS FROM POTASSIUM

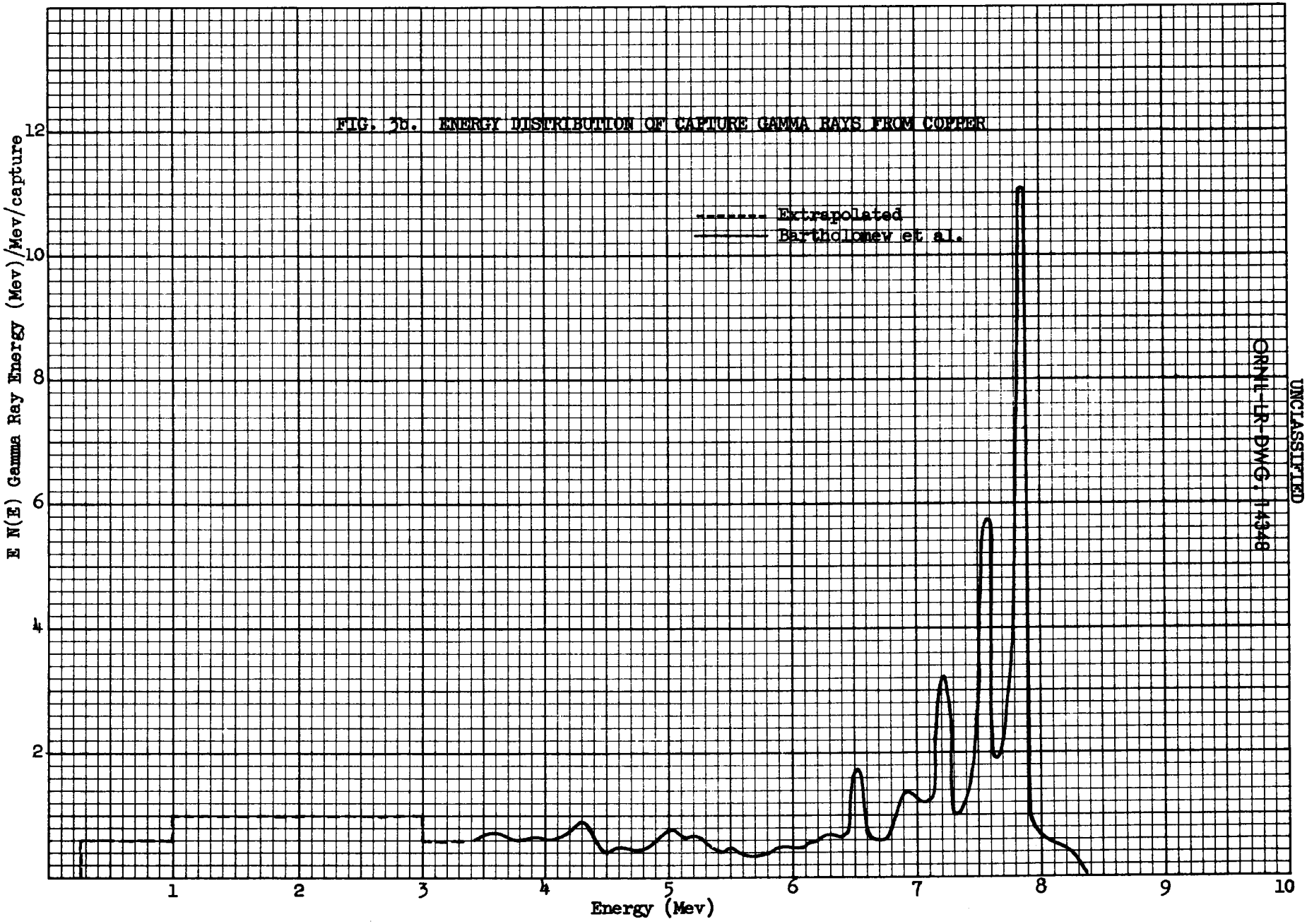
FIG. 3b. ENERGY DISTRIBUTION OF CAPTURE GAMMA RAYS FROM COPPER
Extrapolated
Barthelomew et al.
E N(E) Gamma Ray Energy (Mev)/Mev/capture
Energy (Mev)
ORNL-LR-DWG. 14348
UNCLASSIFIED

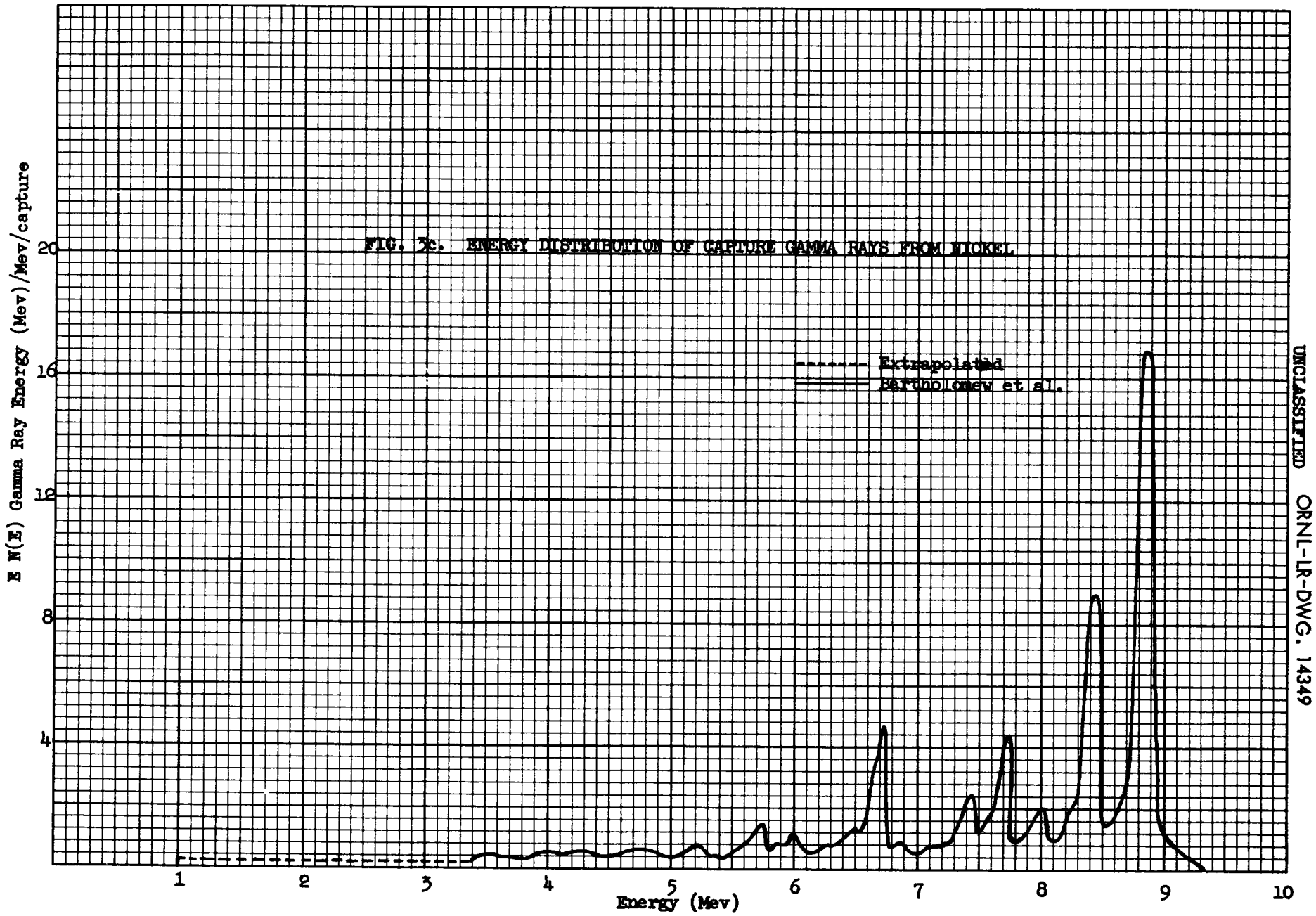

FIG. 3c. ENERGY DISTRIBUTION OF CAPTURE GAMMA RAYS FROM NICKEL

UNCLASSIFIED ORNL-LR-DWG. 14349

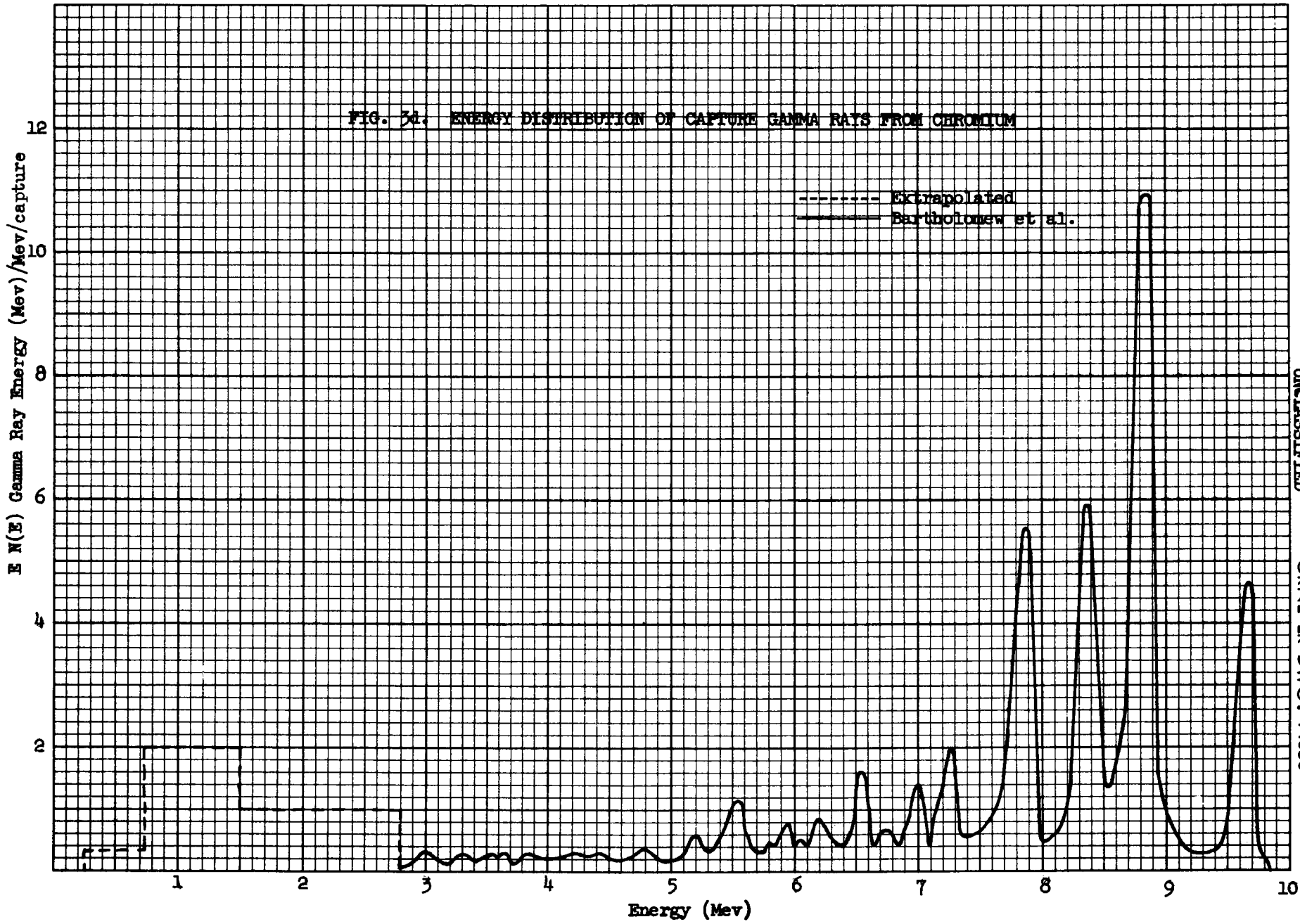

ORNL-LR-DWG. 14350

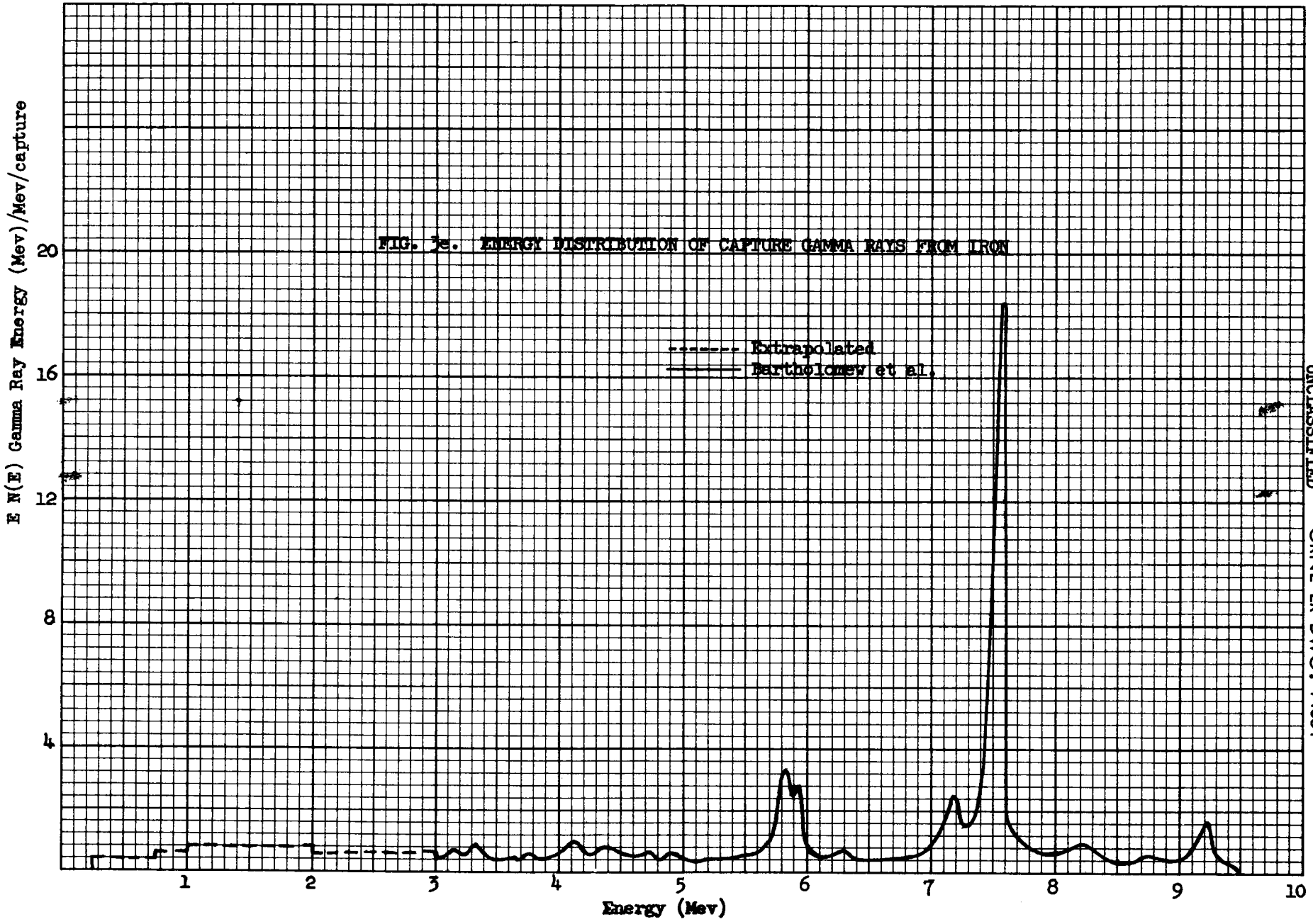

[redacted]

GAMMA RAYS DUE TO INELASTIC SCATTERING OF NEUTRONS

The problem of computing the gamma rays due to the inelastic scattering of neutrons is complicated by the lack of sufficient data. Although a great deal of data on the inelastic cross sections of various elements and materials has accumulated within the last five years, there is comparatively little information on the energy spectra of gamma rays resulting from inelastic scattering.

Graphs of the inelastic cross sections of the various materials which, it is believed, will contribute to the gamma heating in the ART are presented in Figs. 4a to 4k. Also, Table 7 gives the average inelastic cross section for the energy groups used in the multigroup neutron calculations (see Table 8). The references used are indicated on the curves.

In the cases of sodium and fluorine a theoretical formula[25] for the cross section for compound nucleus formation, σ_c, was used over most of the energy range. For high energies, where the capture, elastic, fission, and radiative capture cross sections are usually small, the inelastic cross section approaches the cross section for compound nucleus formation. Fortunately, for fluorine, which is the major contributor in the fuel, there are data available on the inelastic cross section up to 2.2 Mev; above this energy σ_c is a reliable approximation.

The cross sections for iron, nickel, and chromium were obtained from the report of Hughes and Harvey,[4] which gives, for each of these elements, separate cross section curves for each of two energy regions which are roughly from threshold to about 3 Mev[26] and from about 3 Mev to 14 Mev.[27] At about 3 Mev the curves do not join together, so the curves presented here

---

25. J. M. Blatt and V. F. Weisskopf, Theoretical Nuclear Physics, Wiley, New York (1952).
26. R. M. Kiehn and C. Goodman, Phys. Rev. 95, 989 (1954).
27. H. L. Taylor, O. Lönsjö and T. W. Bonner, Phys. Rev. 100, 174 (1955). J. R. Beyster et al., Phys. Rev. 98, 1216 (1955). E. R. Graves and R. W. Davis, Phys. Rev. 97, 1205 (1955); etc.

[redacted]

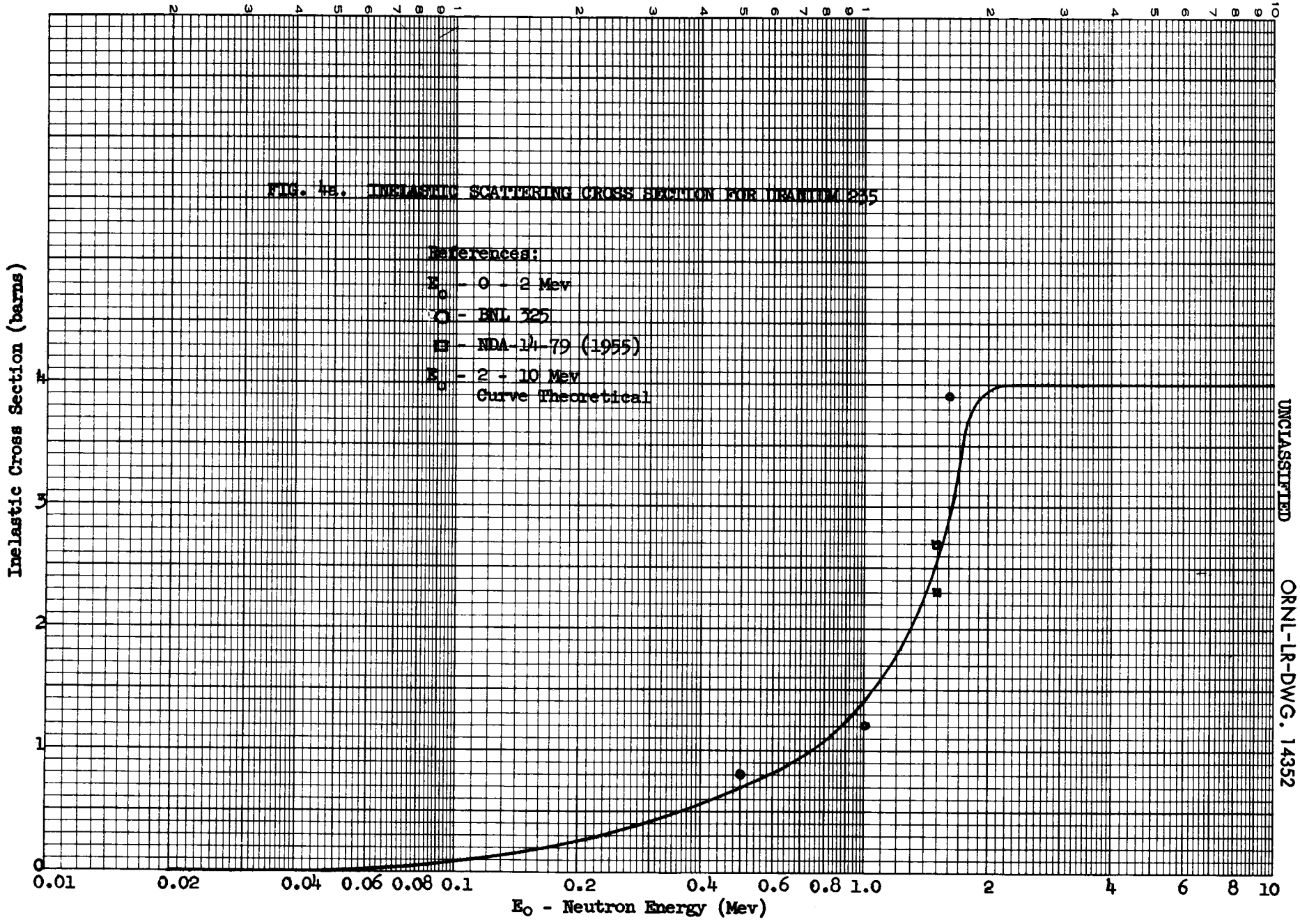

UNCLASSIFIED ORNL-LR-DWG. 14353

FIG. 4b. INELASTIC SCATTERING CROSS SECTION FOR SODIUM

References:

No references found.
Curve is entirely theoretical.[25]

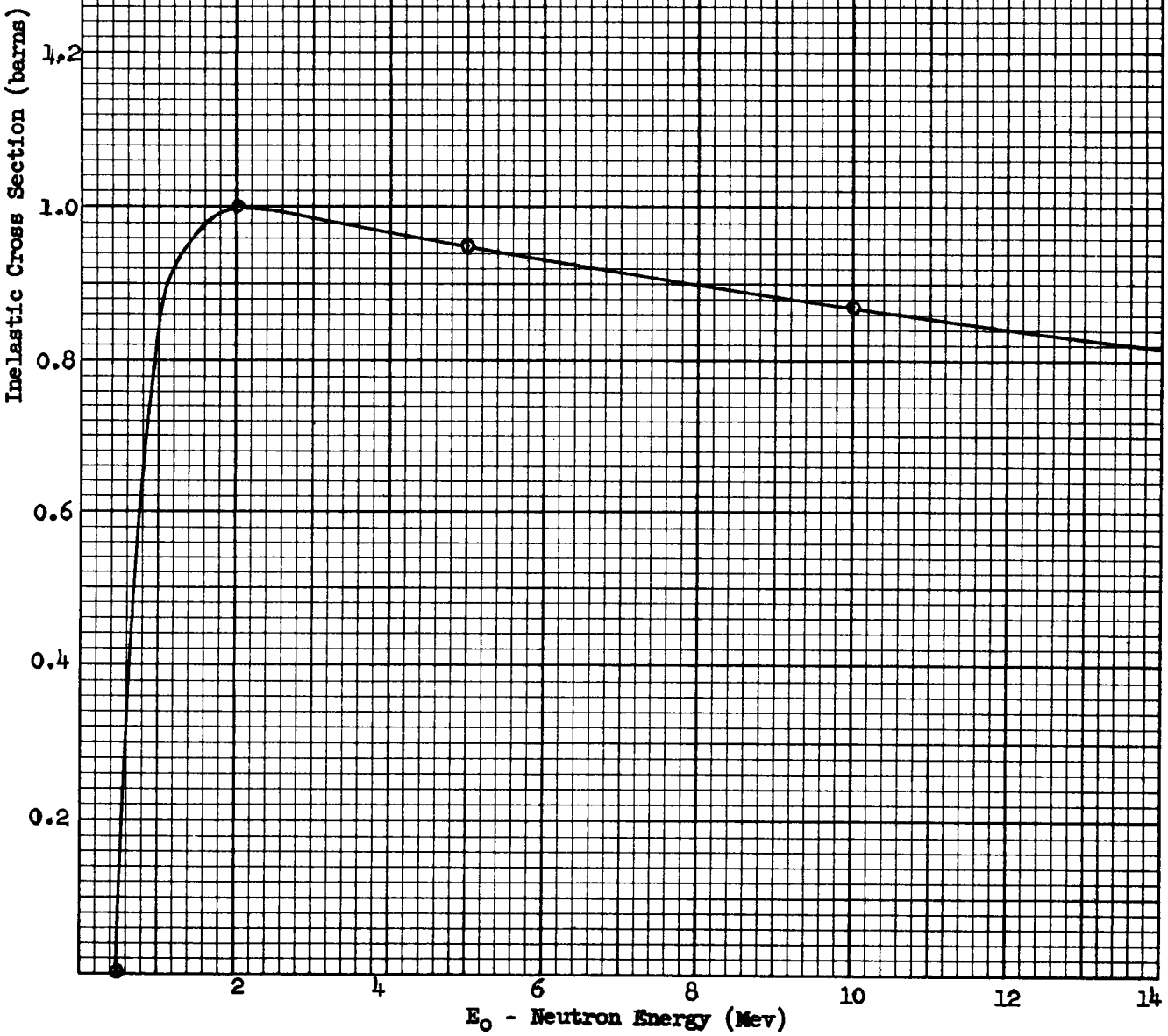

UNCLASSIFIED ORNL-LR-DWG. 14354

FIG. 4c. INELASTIC SCATTERING CROSS SECTION FOR ZIRCONIUM

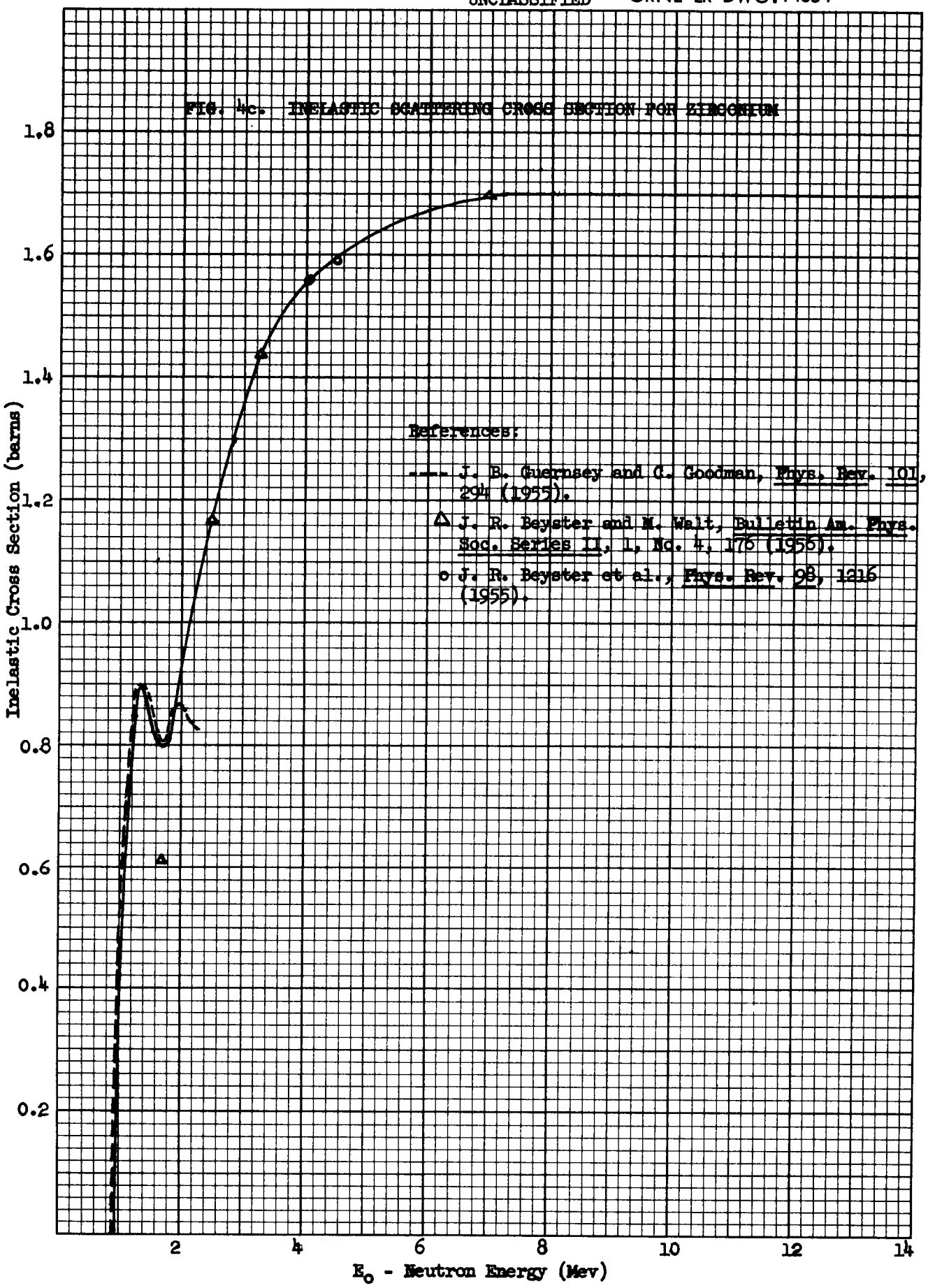

UNCLASSIFIED ORNL-LR-DWG. 14355

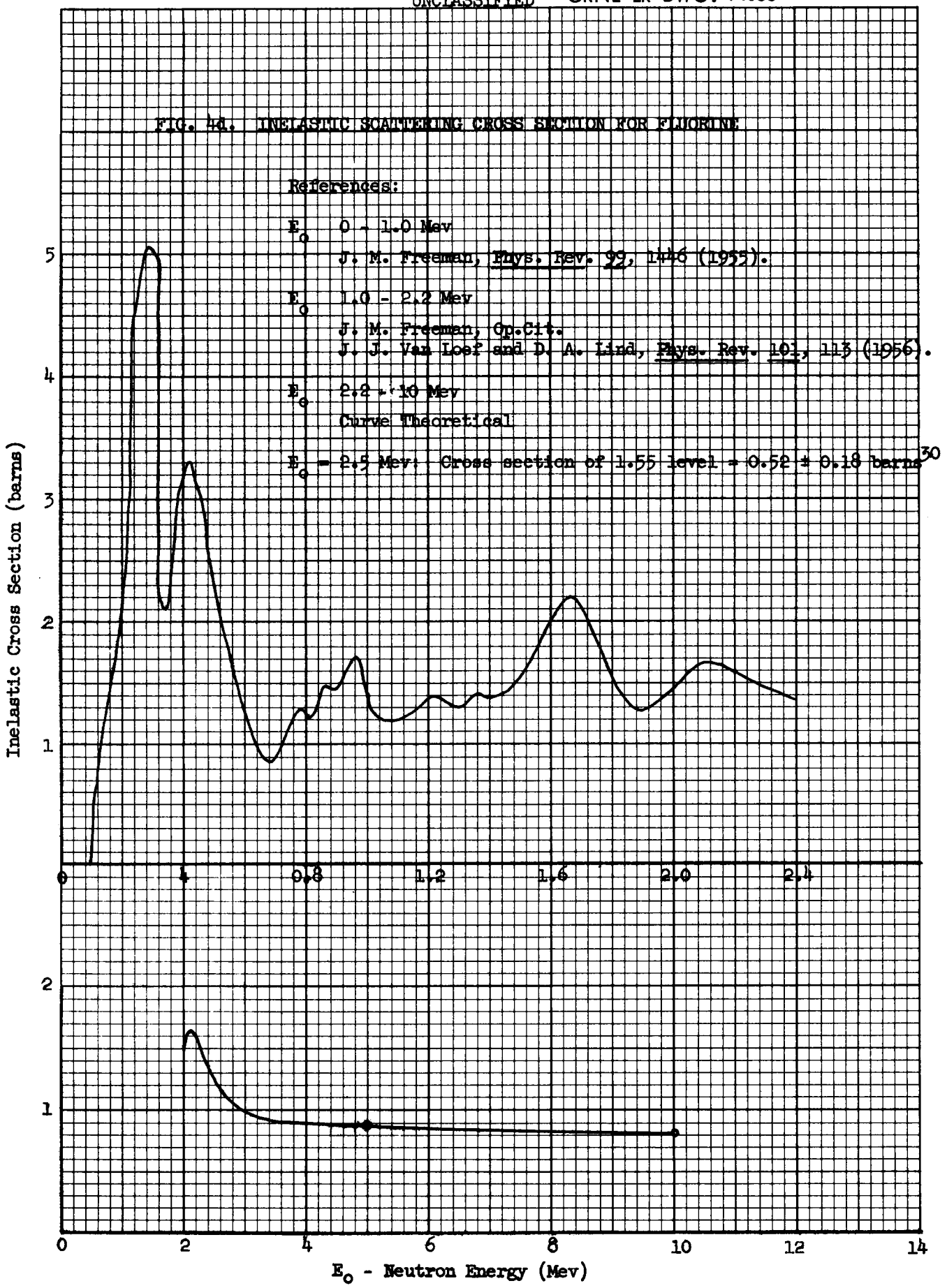

FIG. 44. INELASTIC SCATTERING CROSS SECTION FOR FLUORINE

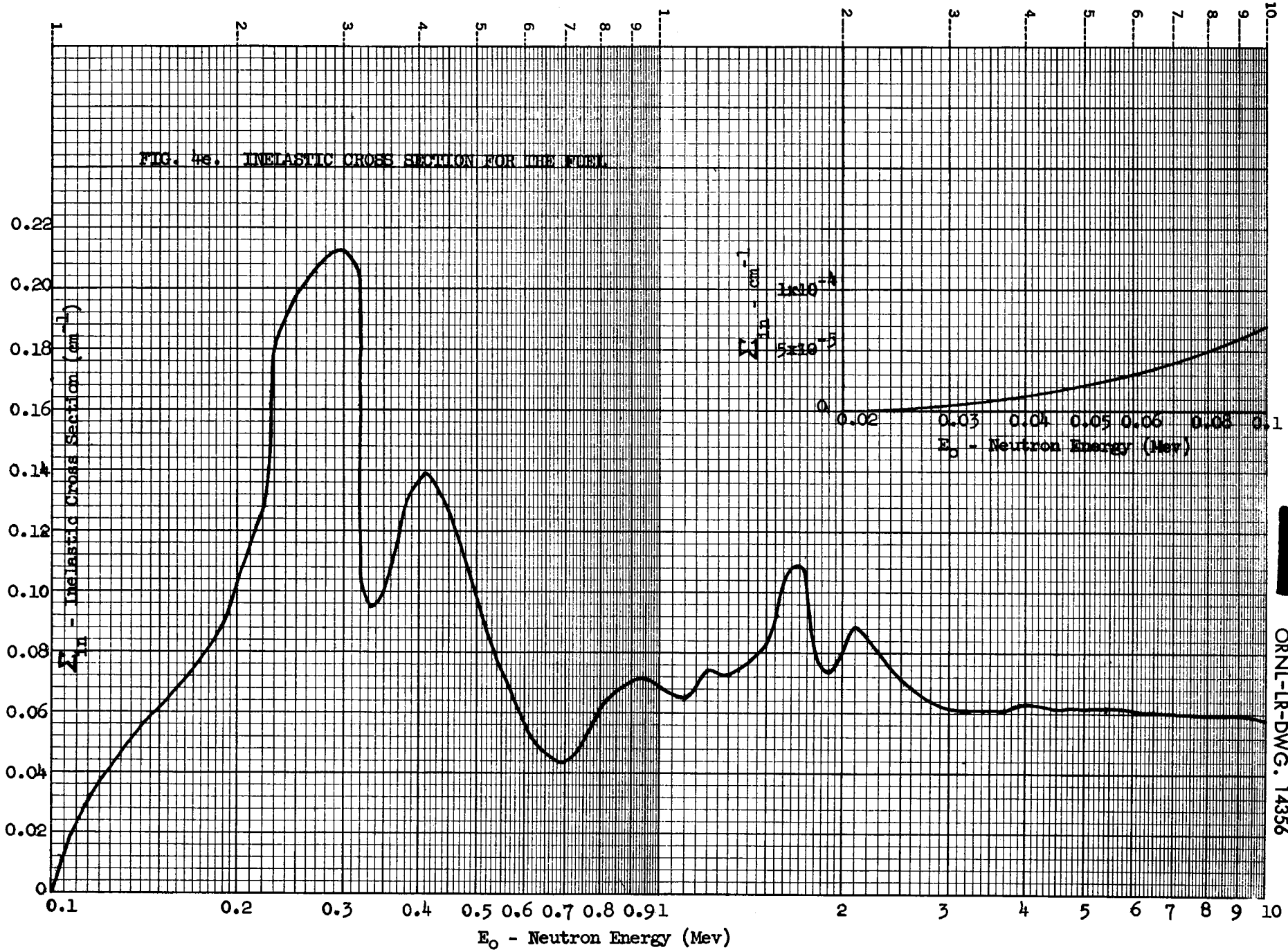
FIG. 46. INELASTIC CROSS SECTION FOR THE FUEL
Σ_{in} - Inelastic Cross Section (cm^{-1})
E_o - Neutron Energy (Mev)
Σ_{in} - cm^{-1}
1x10^{-4}
5x10^{-5}
E_o - Neutron Energy (Mev)
ORNL-LR-DWG. 14356

UNCLASSIFIED ORNL-LR-DWG. 14357

FIG. 4f. NON-ELASTIC SCATTERING CROSS SECTIONS FOR BERYLLIUM

References:

σ(non-elastic) o BNL 325
Δ H. L. Taylor, O. Lonsjo and T. W. Bonner, Phys. Rev. 100, 174 (1955).

σ(n,α) E_o 0 - 5.5 Mev
F. E. Steiscn and E. C. Campbell, Oak Ridge National Laboratory, private communication (1956).
□ M. E. Battat and F. L. Ribe, Phys. Rev. 89, 80 (1953).

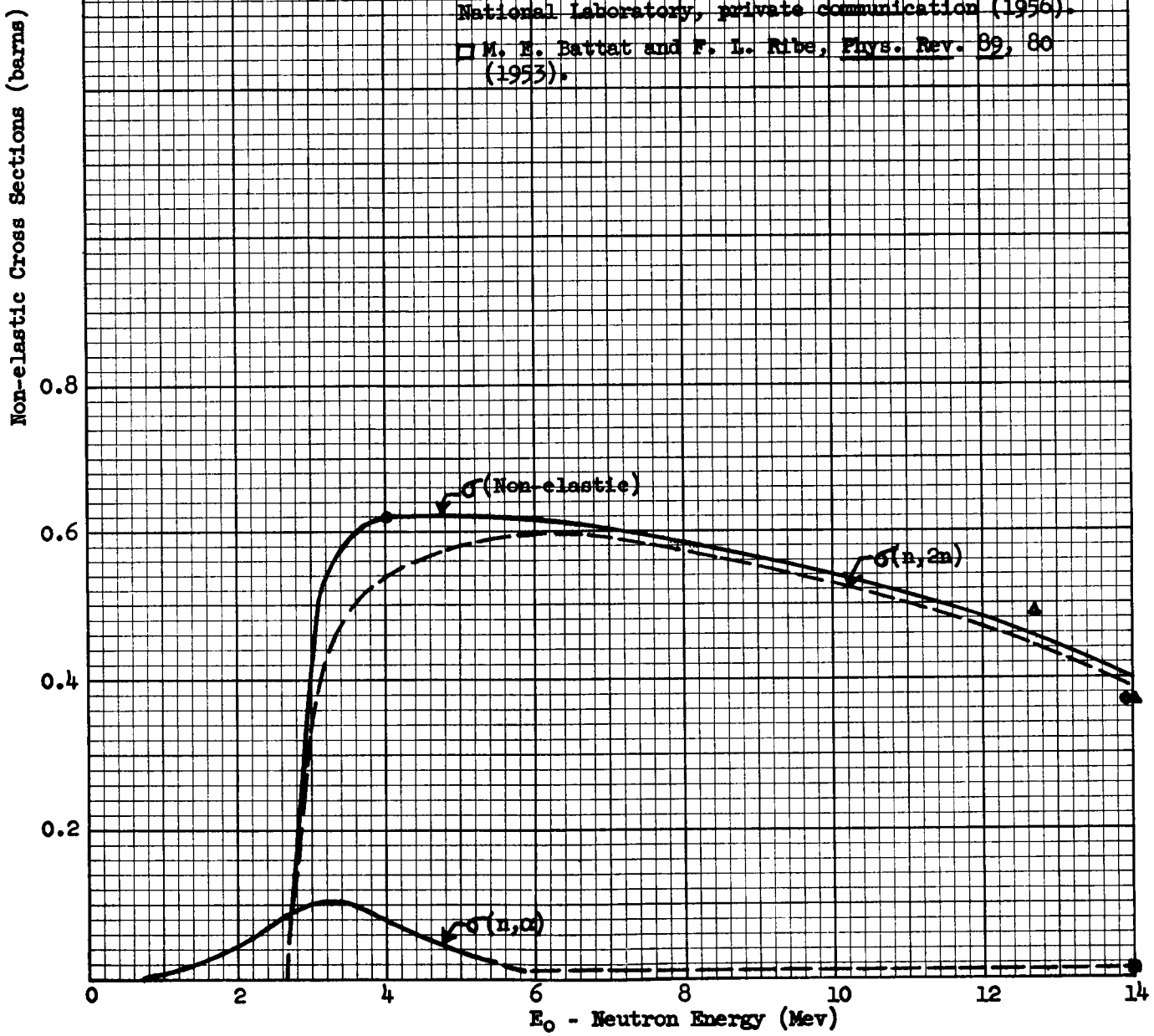

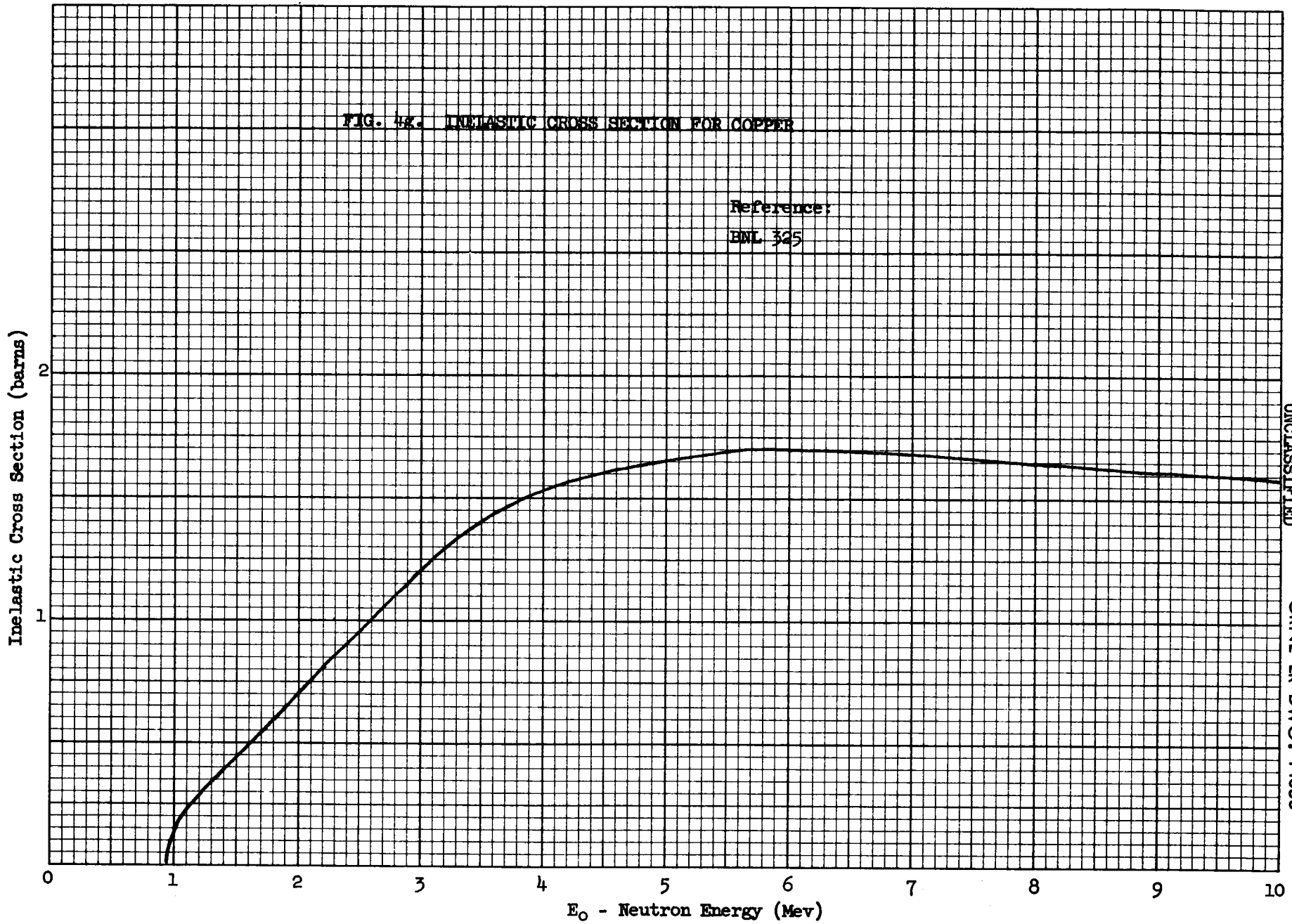

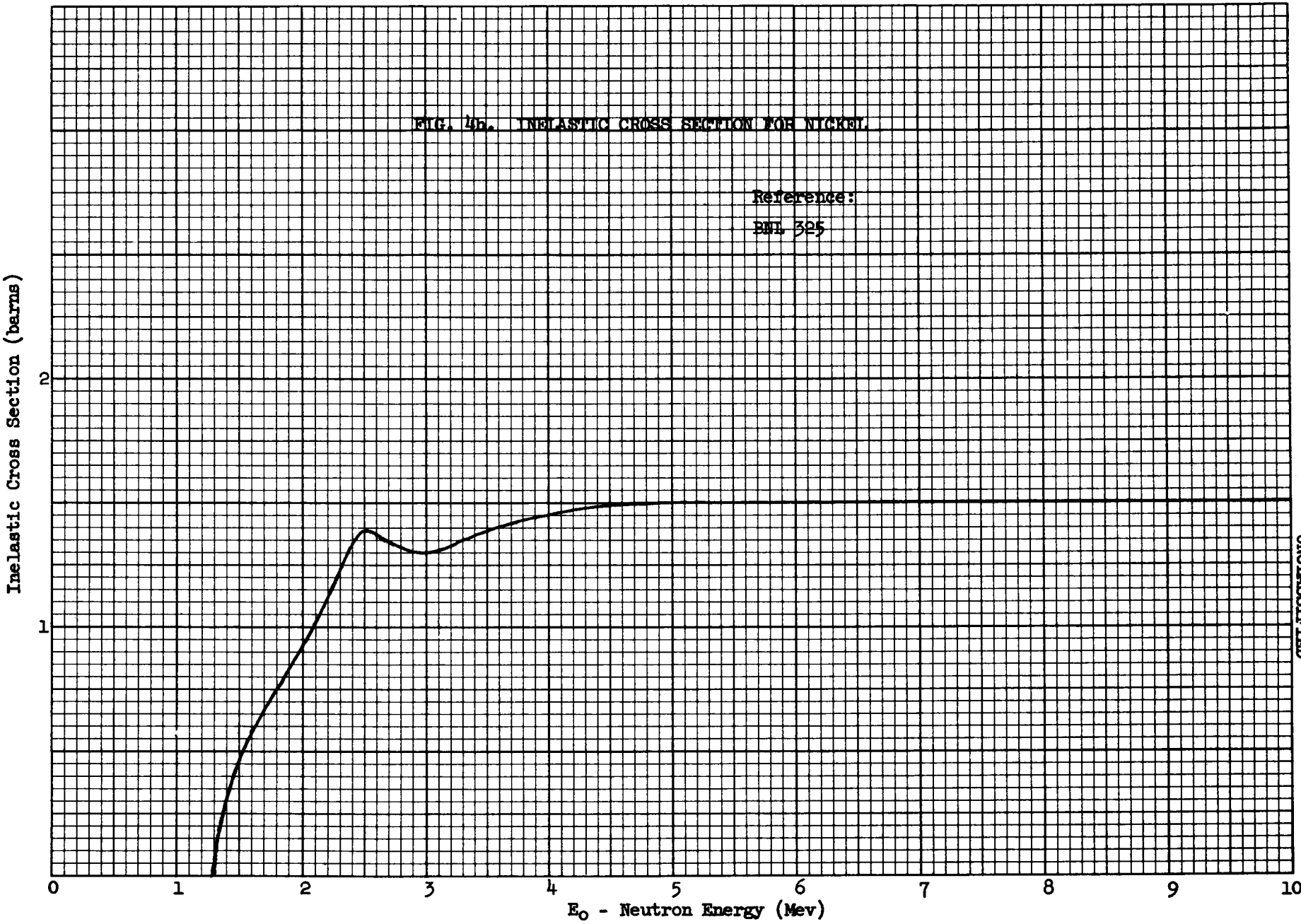

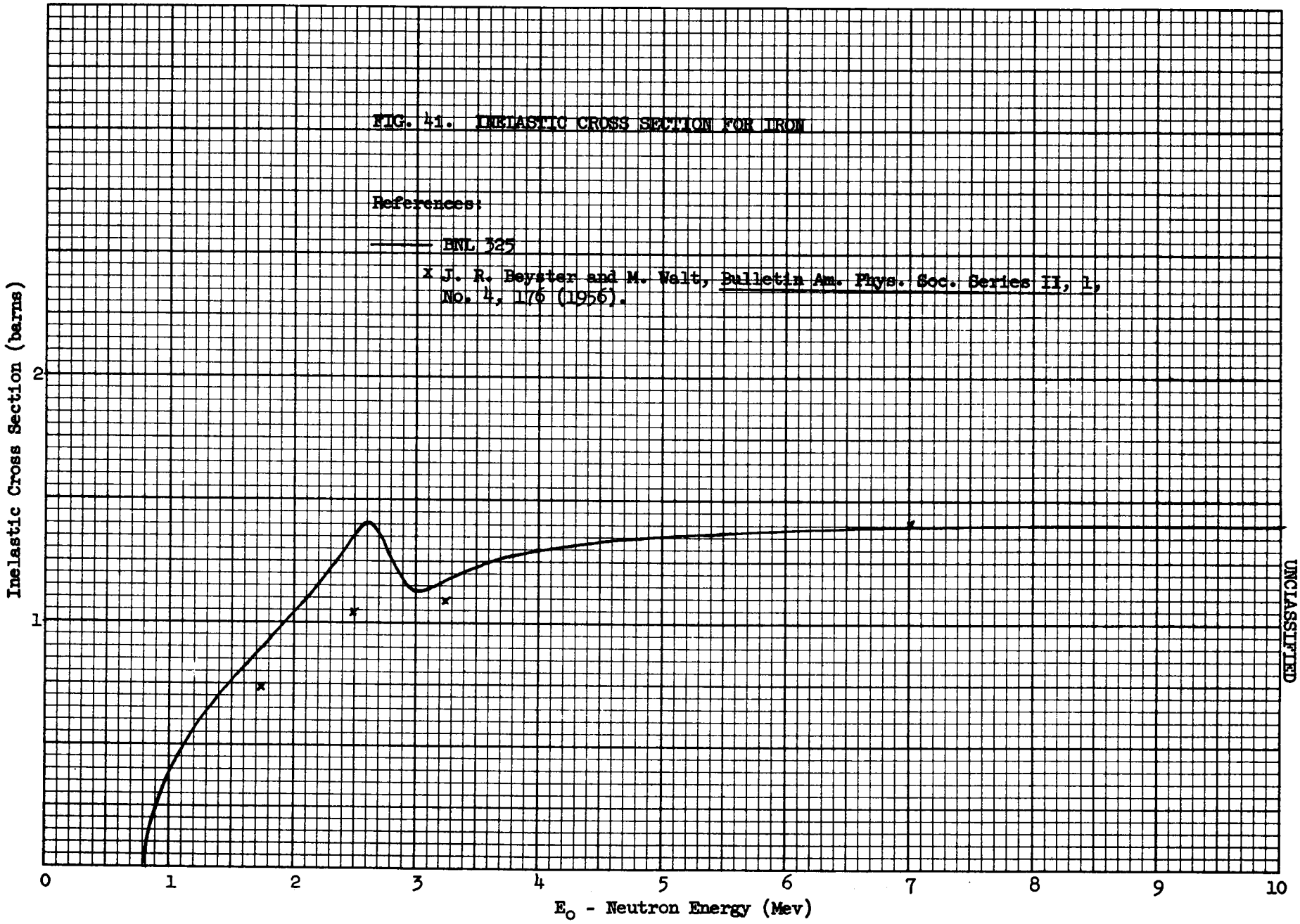

FIG. 41. INELASTIC CROSS SECTION FOR IRON

References:

——— BNL 325

x J. R. Beyster and M. Walt, Bulletin Am. Phys. Soc. Series II, 1, No. 4, 176 (1956).

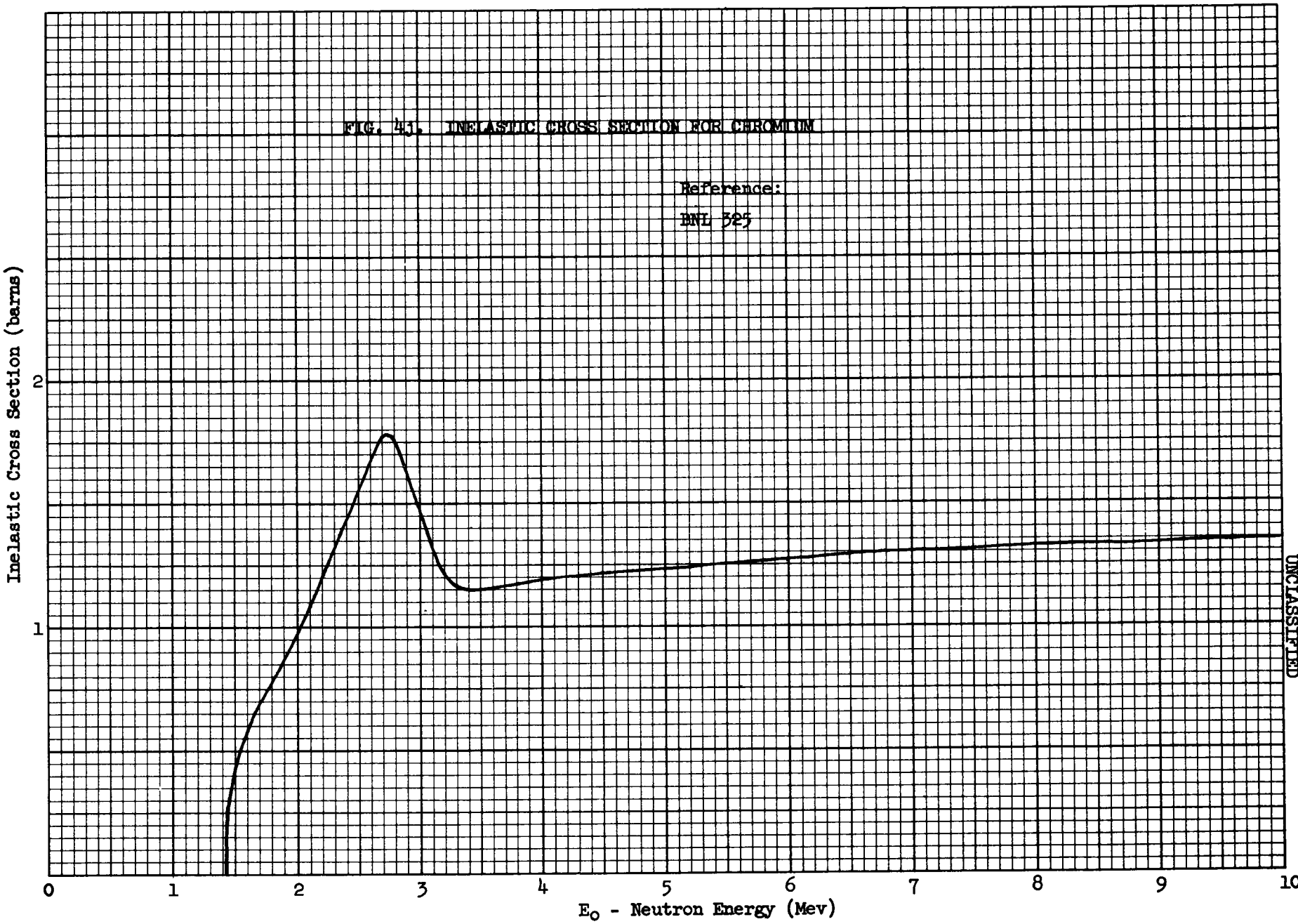

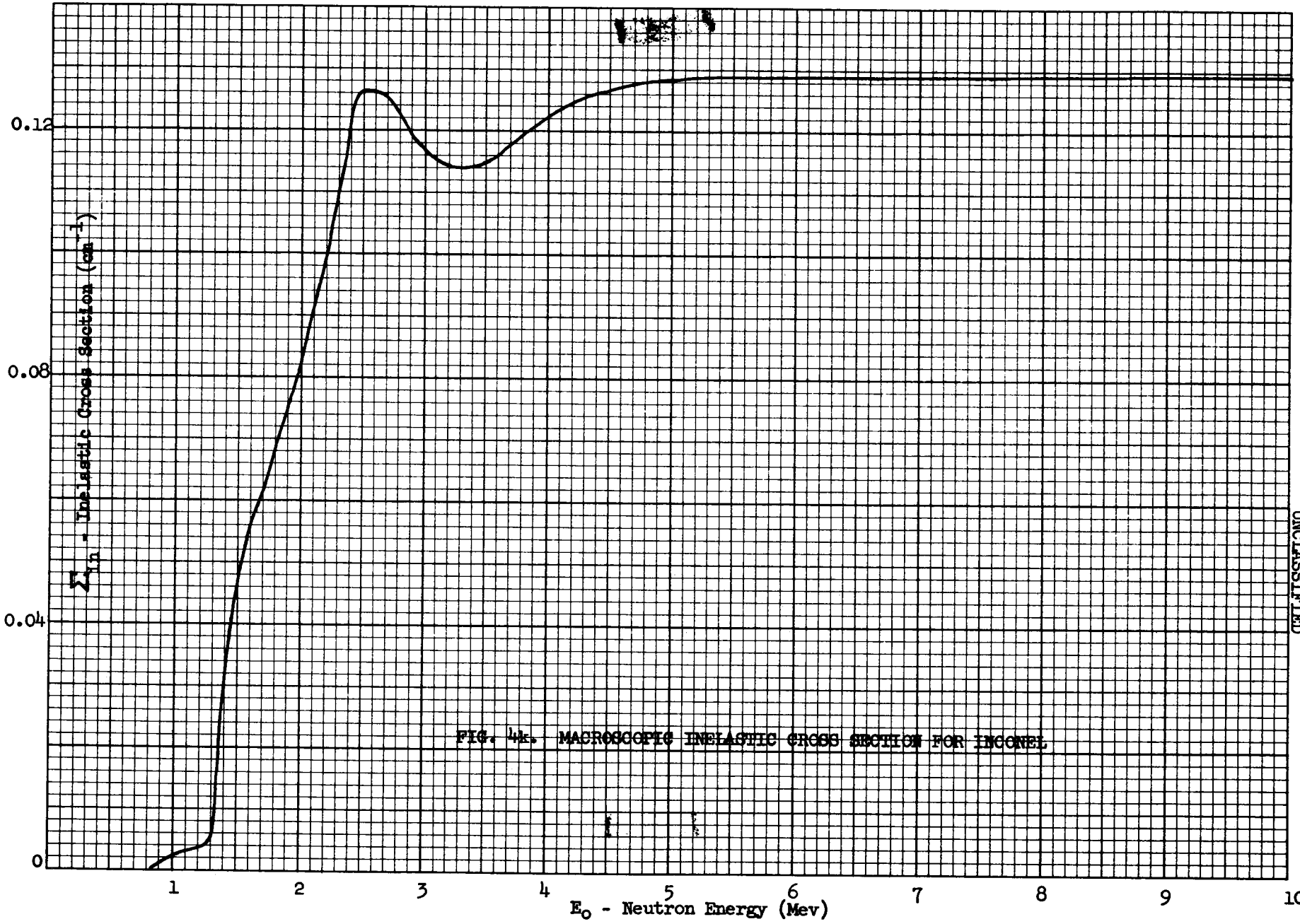

FIG. 4k. MACROSCOPIC INELASTIC CROSS SECTION FOR INCONEL

Table 7. Average Inelastic Cross Sections

Group	$\bar{\sigma}$(barns)								Σ (cm^{-1})	
	U^{235}	Na	Zr	F	Cu	Ni	Fe	Cr	Inconel	Fuel
1	4.0	0.900	1.70	0.830	1.65	1.50	1.40	1.32	0.129	0.060
2	4.0	0.949	1.61	0.885	1.62	1.48	1.34	1.22	0.126	0.062
3	4.0	0.986	1.33	1.08	1.17	1.34	1.26	1.39	0.118	0.065
4	3.37	0.982	0.893	1.65	0.593	0.735	0.914	0.726	0.066	0.085
5	1.58	0.864	0.481	1.45	0.191	0.029	0.431	0	0.0040	0.070
6	0.888	0.403	0	1.30	0	0	0		0	0.058
7	0.558	0		2.84						0.124
8	0.327			3.79						0.166
9	0.086			0.525						0.025
10	0			0						0

[redacted]

Table 8. Multigroup Intervals for Neutron Flux Calculations

Group	Lethargy Limits (u)	Group Width (Δu)	Energy Limits (ev)
1	0 - 0.5	0.5	10^7 - 6.065×10^6
2	0.5 - 1.0	0.5	6.065×10^6 - 3.679×10^6
3	1.0 - 1.5	0.5	3.679×10^6 - 2.231×10^6
4	1.5 - 2.0	0.5	2.231×10^6 - 1.353×10^6
5	2.0 - 2.5	0.5	1.353×10^6 - 0.8208×10^6
6	2.5 - 3.0	0.5	0.8208×10^6 - 0.4979×10^6
7	3.0 - 3.5	0.5	0.4979×10^6 - 0.3020×10^6
8	3.5 - 4.0	0.5	0.3020×10^6 - 0.1832×10^6
9	4.0 - 7.0	3.0	0.1832×10^6 - 0.009118×10^6
10	7.0 - 10.0	3.0	9118 - 454.0
11	10.0 - 11.4	1.4	454.0 - 112.0
12	11.4 - 12.6	1.2	112.0 - 33.72
13	12.6 - 13.4	0.8	33.72 - 15.15
14	13.4 - 13.8	0.4	15.15 - 10.16
15	13.8 - 14.6	0.8	10.16 - 4.564
16	14.6 - 15.8	1.2	4.564 - 1.375
17	15.8 - 16.2	0.4	1.375 - 0.9214
18	16.2 - 16.6	0.4	0.9214 - 0.6176
19	16.6 - 17.0	0.4	0.6176 - 0.4140
20	17.0 - 17.4	0.4	0.4140 - 0.2775
21	17.4 - 17.6	0.2	0.2775 - 0.2272
22	17.6 - 17.8	0.2	0.2272 - 0.1860
23	17.8 - 18.0	0.2	0.1860 - 0.1523
24	18.0 - 18.2	0.2	0.1523 - 0.1247
25	18.2 - 18.4	0.2	0.1247 - 0.1021
26	18.4 - 18.6	0.2	0.1021 - 0.08358
27	18.6 - 18.8	0.2	0.08358 - 0.06843
28	18.8 - 19.0	0.2	0.06843 - 0.05603
29	19.0 - 19.2	0.2	0.05603 - 0.04587
30	19.2 - 19.4	0.2	0.04587 - 0.03756
31	19.4 - 19.6	0.2	0.03756 - 0.03075
32	19.6 - 19.8	0.2	0.03075 - 0.02518

Thermal Group	Lethargy	Temperature, (°F)	Energy (ev)
25	18.4	1672	0.1021
26	18.6	1283	0.08358
31	19.6	183	0.03075
32	19.8	66	0.02518

[redacted]

[redacted]

are approximately an average value of the experimental points in this region. Very recent work on iron by Beyster and Walt[28] in the energy range from 1.75 to 7 Mev gives experimental points which are fairly close to the curve presented in Fig. 4i. The maximum difference is at 2.5 Mev where their value is about 25% lower than the curve of Fig. 4i. The inelastic cross section curve for copper was also taken from the work of Hughes and Harvey.[4]

The threshold values for inelastic scattering were obtained from the work of Way et al.,[29] and Ajzenberg and Lauritsen.[30] The graphs of the macroscopic inelastic cross section of the fuel and of Inconel as functions of the incident neutron energy were obtained by summing the macroscopic cross sections of the constituents of each.

Discussion

Inelastic scattering of neutrons is a two-step process. First, the incident neutron is captured into one of the levels of the target nucleus forming a compound nucleus which then decays, by neutron emission, leaving the nucleus in an excited state from which it decays to the ground state by the emission of one or more gamma rays. The emergent neutron has an energy essentially equal to the incident neutron energy minus the excitation energy of the residual nucleus. This assumes that the kinetic energy acquired by the nucleus (recoil energy) is negligible and thus that inelastic neutron heating can be neglected for all but the lightest elements ($A < 12$).

Weisskopf[31] showed that the spectrum of the inelastically scattered neutron can be represented by

$$F(E_n)\, dE_n = C\, E_n\, e^{-E_n/T}\, dE_n ,$$

28. J. R. Beyster and M. Walt, Bulletin of the American Phys. Soc. Series II, 1, No. 4, 176 (1956).
29. K. Way, R. W. King, C. L. McGinnis and R. van Lieshout, Nuclear Level Schemes, TID-5300 (June, 1955).
30. F. Ajzenberg and T. Lauritsen, Rev. Mod. Phys. 24, 321 (1952).
31. V. F. Weisskopf, Phys. Rev. 52, 295 (1937).

[redacted]

[redacted]

where

E_n = inelastically scattered neutron energy, Mev,

$F(E_n)\,dE_n$ = fraction of neutrons scattered into the energy interval between E_n and $E_n + dE_n$,

T = nuclear temperature.

Weisskopf's statistical model is applicable under the conditions that the incident neutron energy is large compared with the level spacing of the residual nuclei and that the incident neutron energy is distributed among all the nucleons of the target nucleus. This model neglects the effects of spin and parity of the various excited levels of the compound nucleus and assumes continuously varying energy density of the levels in the residual nucleus. Thus, this model should not be used for light elements ($A < 12$) or low incident neutron energies ($E_o < \sim 3$ Mev). For incident neutron energies smaller than 3 Mev, the average neutron energy loss per inelastic collision ($E_o - \overline{E}_n$), has been obtained in most cases from experimental data. (In the preceding sentence, $E_o \equiv$ incident neutron energy, $\overline{E}_n \equiv$ average energy of inelastically scattered neutrons.)

Derivation of Formula for High Incident Neutron Energies

Let

$$\delta_{in}(E_o,A) \equiv \frac{E_{\gamma t}}{E_o} = \frac{E_o - E_n}{E_o},$$

where

$E_{\gamma t}$ = total gamma-ray energy emitted (the average photon energy $\overline{E}_\gamma$ may be considerably less),

and let

$T(E_o,A) \equiv$ nuclear temperature.

As

$$F(E_n)\,dE_n = C\,E_n\,e^{-E_n/T}\,dE_n,$$

[redacted]

[redacted]

where

$$C = \left\{ T^2 \left[1 - (1 + E_o/T)\, e^{-E_o/T} \right] \right\}^{-1} ,$$

since

$$\int_o^{E_o} F(E_n)\, dE_n = 1 .$$

Let

$$\Delta E = E_o - E_n ,$$

$$\overline{\Delta E} = \int_o^{E_o} \Delta E\, F(E_n)\, dE_n = E_o - \overline{E_n} ,$$

$$\delta_{in} = \frac{\overline{\Delta E}}{E_o} = \frac{e^{-E_o/T} (1 + 2T/E_o) + 1 - 2T/E_o}{1 - (1 + E_o/T)\, e^{-E_o/T}} .$$

For $E_o/T > 5$, this expression essentially reduces to

$$\delta_{in} \simeq 1 - 2T/E_o$$

and $\overline{E_n} = 2T$.

At sufficiently high incident neutron energies two neutrons may be emitted. This (n,2n) reaction can be considered as a double inelastic scattering. When the surplus of incident energy E_o, over the threshold of the (n,2n) reaction becomes large, the cross section for the (n,2n) reaction, $\sigma(n,2n)$, will approach the cross section for the formation of a compound nucleus, σ_c. The effect of the (n,2n) reaction will be to reduce δ_{in} and $\overline{E}_\gamma$. Paul and Clarke[32] have measured $\sigma(n,2n)$ for a number of elements and showed that there was good agreement with the calculated

32. E. B. Paul and R. L. Clarke, Can. J. Phys. 31, 267 (1953).

[redacted]

[redacted]

values of $\sigma(n,2n)$ obtained by using Weisskopf's formula:[25]

$$\sigma(n,2n) \simeq \sigma_c \left[1 - \left(1 + \frac{E_o - E_b}{T}\right) e^{-(E_o - E_b)/T}\right],$$

where

T = temperature of residual nucleus after emission of first neutron.

E_b = threshold for (n,2n) reaction (essentially equal to binding energy of the second neutron).

Graves and Rosen[33] measured the inelastic neutron spectrum for the interaction of 14-Mev neutrons with a number of elements whose (n,2n) thresholds are about 10 Mev or higher. For 14-Mev incident neutrons the maximum energy of the residual nucleus after emission of the first neutron is usually high enough so that the energy of the second emergent neutron will have a Maxwellian distribution characterized by a temperature $T(E_o - E_b)$. Thus the inelastic neutron spectra will be represented by the sum of two exponentials, the relative proportions of each being determined by the cross sections of the (n,n') and (n,2n) reactions. Although none of the elements investigated showed evidence of a second exponential, both exponentials are probably present for the heavier elements, i.e., U^{235}, and Graves and Rosen stated that the resolution in their experiment was probably not good enough to separate the two exponentials.

A list of E_b, $\sigma(n,2n)$, and the non-elastic cross sections for 14-Mev neutrons for the different elements in the fuel, Inconel, and beryllium are given in Table 9.

From Table 9 it can be seen that the (n,2n) reaction is important only in the case of U^{235} and Be^9. The effect of the (n,2n) reaction, of course, is to reduce the energy that appears in the form of gamma radiation. In the case of U^{235}, the (n,2n) cross section is a small part of the total

---

33. E. R. Graves and L. Rosen, LA-1532 (1953), Secret.

[redacted]

[redacted]

Table 9. Values for $E_b(n,2n)$, $\sigma(n,2n)$, and Non-elastic Cross Sections for 14-Mev Neutrons

Element	$E_b(n,2n)$ (Mev)	$\sigma(n,2n)$ at 14 Mev (barns)	σ(Non-elastic) at 14 Mev[a] (barns)
F^{19}	11.0[b]	0.060[c]	0.75
Na^{23}	12.8[b]	0.020[d]	0.82
Zr^{90}	12.5[e]	0.080[c]	1.70
U^{235}	5.4[b]	0.4 ± 0.3[f,g]	4.0
Ni^{58}	11.9[b]	0.040[c]	1.50
Fe^{56}	11.5[b]	~0.04 from Ni	1.40
Cr^{52}	11.8[e]	~0.04 from Ni	1.40
Be^{9}	1.85[b]	0.3 - 0.5[h]	0.40
Cu	10.4[i]	0.55[i]	1.45[i]

[a] Values taken from σ_{in} curves.

[b] $E_b(n,2n) = \frac{A+1}{A}$ (binding energy[g] of last neutron in target nucleus).

[c] E. B. Paul and R. L. Clarke, Can. J. Phys. 31, 267 (1953).

[d] Calculated from Weisskopf formula.

[e] B. T. Feld et al., NYO-636 (1951).

[f] Value of U^{238} used for that of U^{235}.

[g] Reactor Handbook, Vol. 1, Tables 1.2.3, 1.2.16 (1955).

[h] Preliminary average value, threshold to 14 Mev. Private communication from P. Byerly, University of California Radiation Laboratory, to A. M. Perry.

[i] D. J. Hughes and J. A. Harvey, Neutron Cross Sections, BNL-325 (July 1, 1955).

[redacted]

[redacted]

inelastic cross section. The effect was taken into account by arbitrarily doubling the nuclear temperature characterizing the emitted single neutron spectrum, thereby reducing by a few percent the energy available for gamma radiation. Fortunately U^{235} is not a major contributor to the total gamma-ray source strength from inelastic scattering in the ART.

As there is no true inelastic cross section for Be^9 in the energy range of interest, an (n,2n) cross section was obtained by subtracting $\sigma(n,\alpha)$ from σ(non-elastic). The available experimental data for the Be^9 (n,2n) reaction[30] indicate that for $E_o < 6.8$ Mev, the principal reaction appears to involve a cascade process $\left[Be^9 (n,n') Be^{9*} \longrightarrow Be^8 + n''\right]$. Apparently for $6.8 \leqslant E_o < 10$ Mev, the excited state of Be^9 can also result in alpha particle emission $\left[Be^9 (n,n') Be^{9*} \longrightarrow He^5 + \alpha\right]$. As Be^8 breaks up into alpha particles and He^5 into an alpha particle and a neutron, the two main (n,2n) reactions apparently result in the same end products as follows:

$$Be^9 + n \longrightarrow n' + Be^{9*} \qquad Be^{9*} \begin{cases} \nearrow Be^8 + n'' \longrightarrow 2\alpha + n'' \\ \searrow He^5 + \alpha \longrightarrow 2\alpha + n'' \end{cases}$$

Thus, there appears to be very little possibility for gamma radiation from a Be^9 (n,2n) reaction below 10 Mev, and in fact, no gamma rays have been reported below 3.2 Mev.[34]

Weisskopf, on a theoretical basis, obtained the following expression for the nuclear temperature

$$T = \left(\frac{E_o}{a}\right)^{1/2},$$

where a is a function of the atomic number. This expression assumes an exponential level density and that the incident neutron energy is distributed among all the nucleons of the target nucleus. The available measurements on the spectra of inelastically scattered neutrons[33,35] show a nuclear

34. V. E. Scherrer, B. A. Allison and W. R. Faust, Phys. Rev. 96, 387 (1954).
35. F. E. Bjorklund, LRL-84 (1954).

[redacted]

[redacted]

temperature lower than the theoretical value. It appears therefore that the level density near the ground state increases more slowly with energy than is indicated by the exponential, while at higher energies the level density tends to increase faster than the exponential. The combined effect is to decrease the dependence of the nuclear temperature on incident neutron energy. Graves and Rosen[33] have obtained the nuclear temperature T, for 14-Mev neutrons, for a number of elements, by plotting

$$\ln\left[\frac{F(E_n)}{E_n}\right] \text{ vs } E_n \ .$$

As shown in Fig. 5, T depends rather weakly upon the atomic weight, A. This fact, combined with the observation that the penetrability of the nuclear surface is almost unity if $E_o > 10$ Mev,[25] indicates that the neutron probably leaves the compound nucleus before it has shared its energy with all the nucleons. Bjorklund[35] found that T does not vary as $\sqrt{E_o}$ and, in general, is relatively insensitive to E_o.

Since δ_{in} can be obtained below $E_o = 3$ Mev for a number of elements from experimental data, and an upper limit of δ_{in} at 14 Mev is known,[33] δ_{in} was obtained between 3 and 14 Mev from the formula based on the statistical model and by extrapolating where necessary to give a smooth fit with experimental data. Where experimental data were not available at low energies, the curve based on the statistical model was extrapolated to the lowest inelastic scattering threshold. The values of δ_{in} as a function of E_o for the various constituents of the fuel, Inconel, and copper are shown in Figs. 6a through 6e. On the basis of the data presently available on nuclear temperature and the known extremes of δ_{in} vs E_o, T was assumed to be independent of E_o, and the values of T used were obtained from the curve of T vs A (determined at 14 Mev) for the elements with mass numbers between 12 and 210. In the case where T is assumed to be dependent on E_o and has been obtained for those few elements whose inelastic neutron spectra have been measured and found to be Maxwellian at $E_o = 3$ Mev, the resulting δ_{in} would be 10% higher at $E_o = 3$ Mev, which represents the worst condition, than the δ_{in} obtained by assuming T to be independent of E_o. As an example, T of tungsten

[redacted]

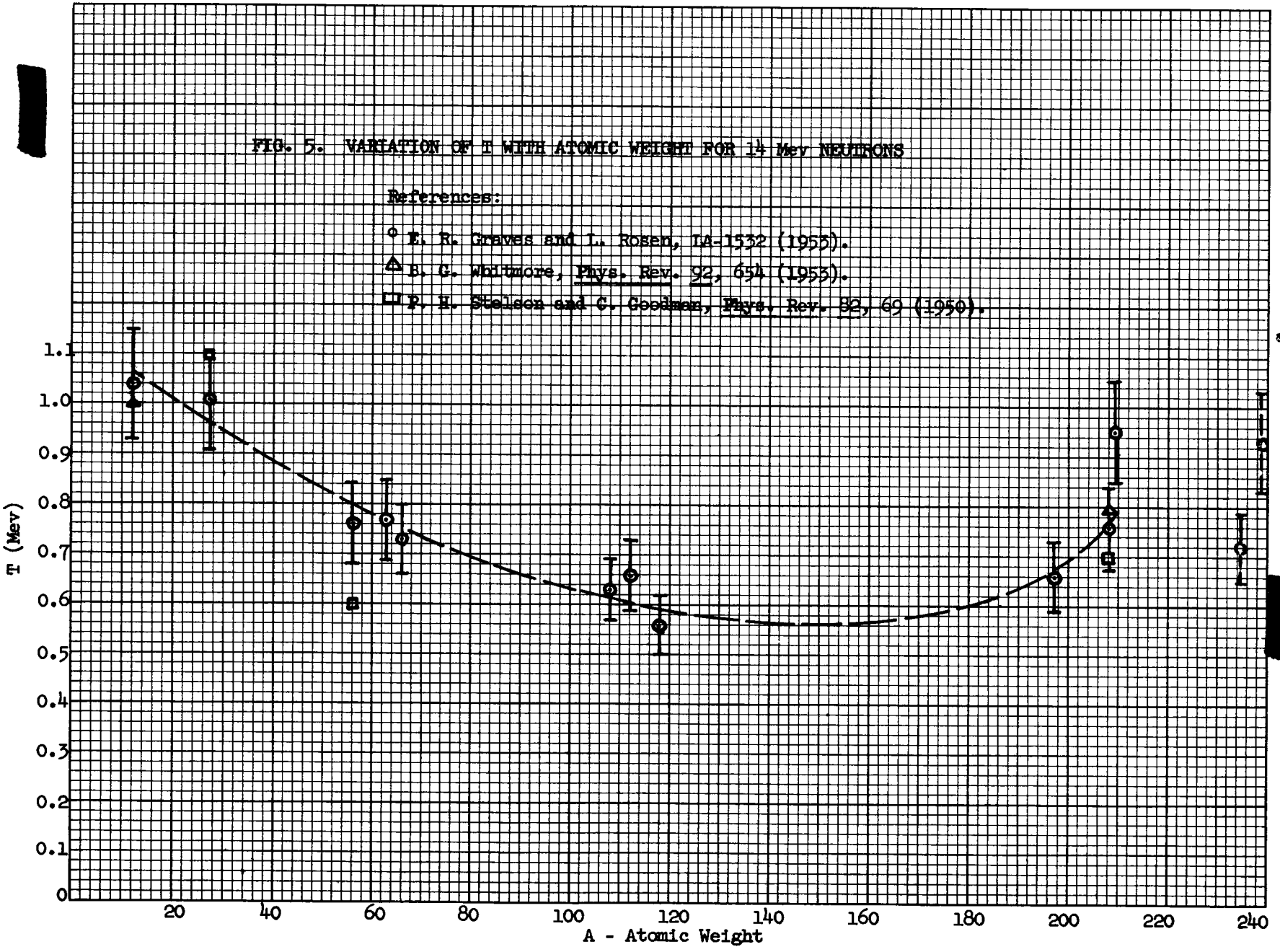

FIG. 5. VARIATION OF T WITH ATOMIC WEIGHT FOR 14 Mev NEUTRONS

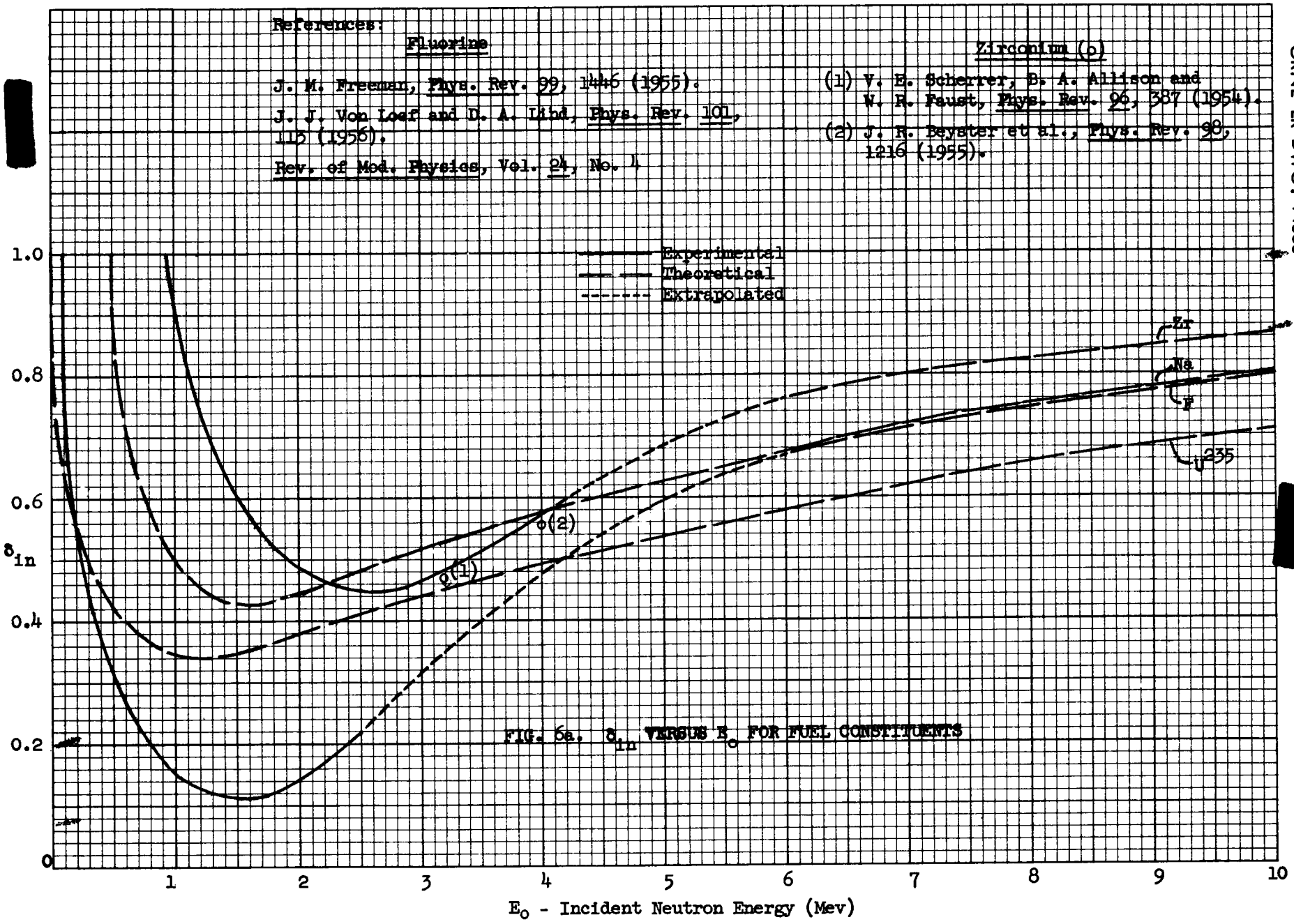

FIG. 6a. δ_{in} VERSUS E_o FOR FUEL CONSTITUENTS

ORNL-LR-DWG. 14363

FIG. 6b. $\overline{\delta}_{in}$ VERSUS E_o FOR FUEL

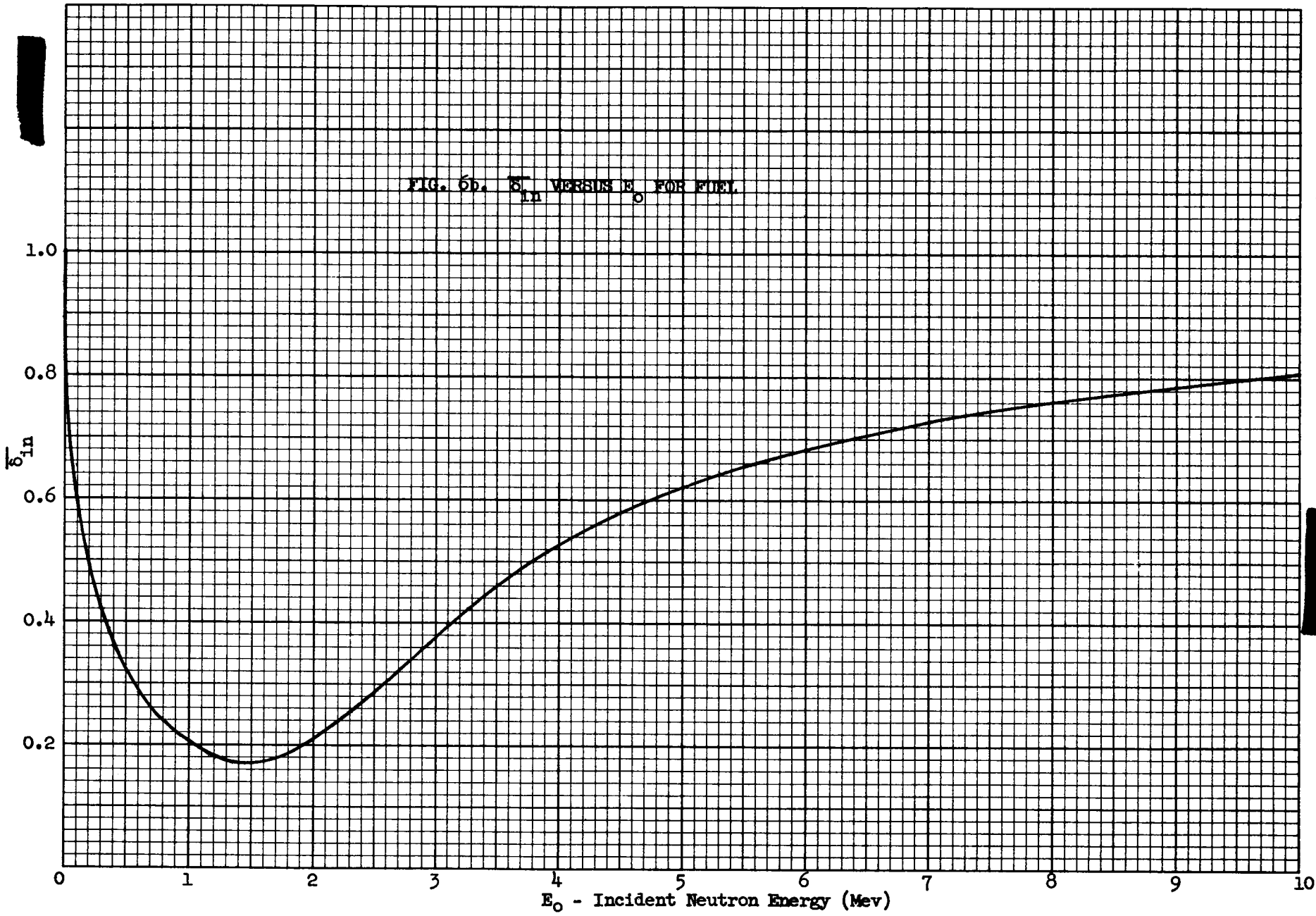

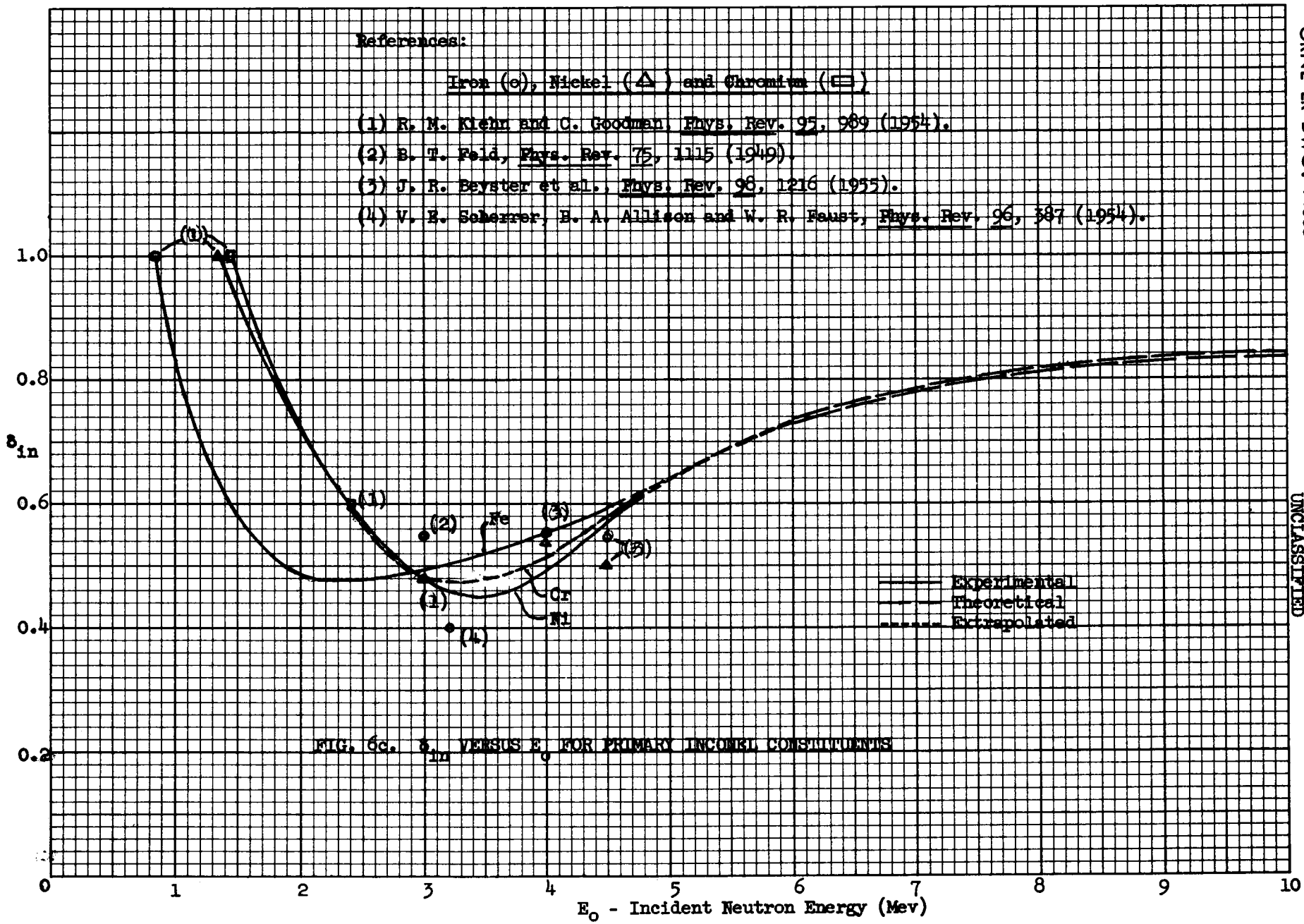

FIG. 6c. δ_{in} VERSUS E_o FOR PRIMARY INCONEL CONSTITUENTS

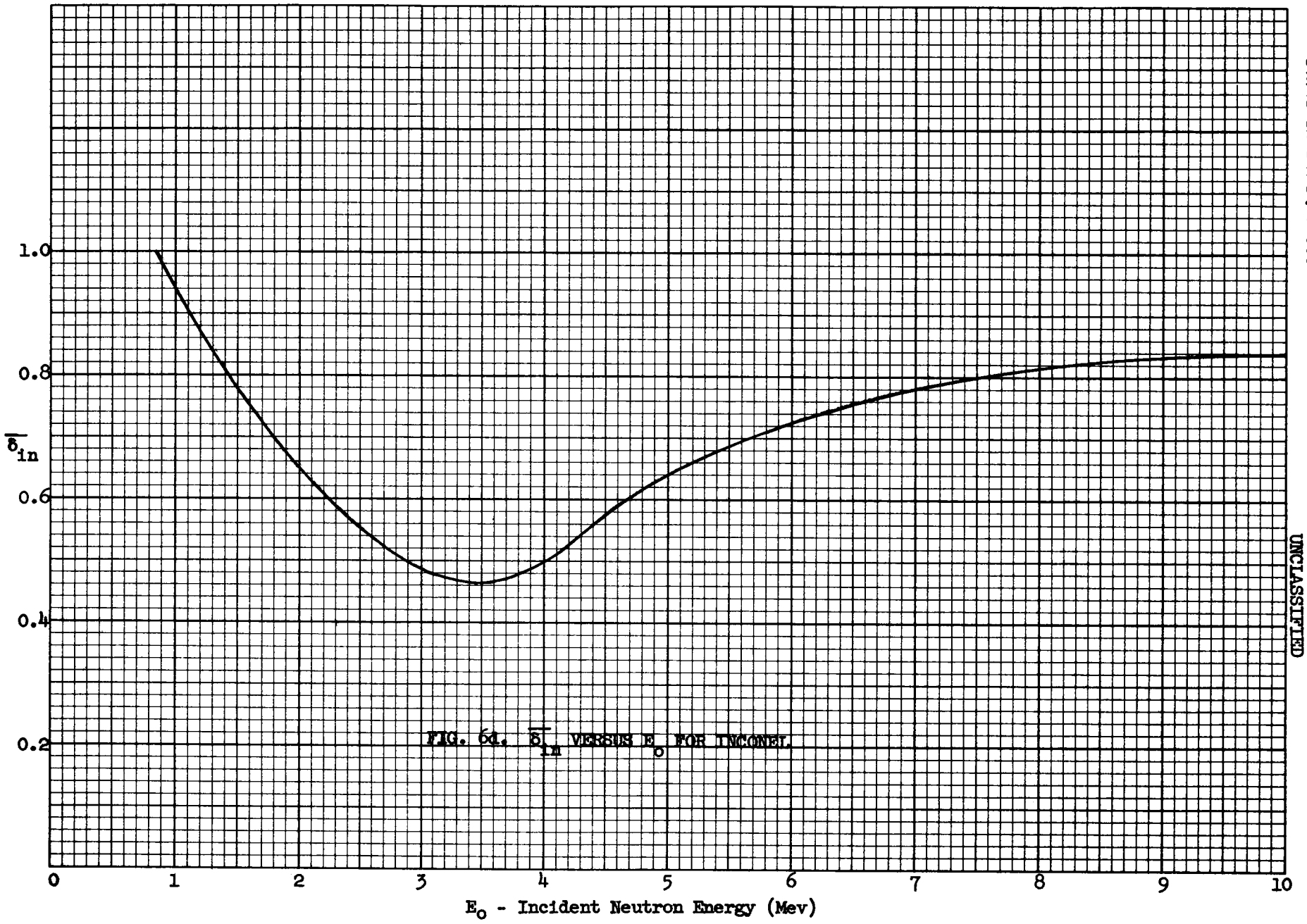

FIG. 64. $\overline{\delta}_{in}$ VERSUS E_o FOR INCONEL

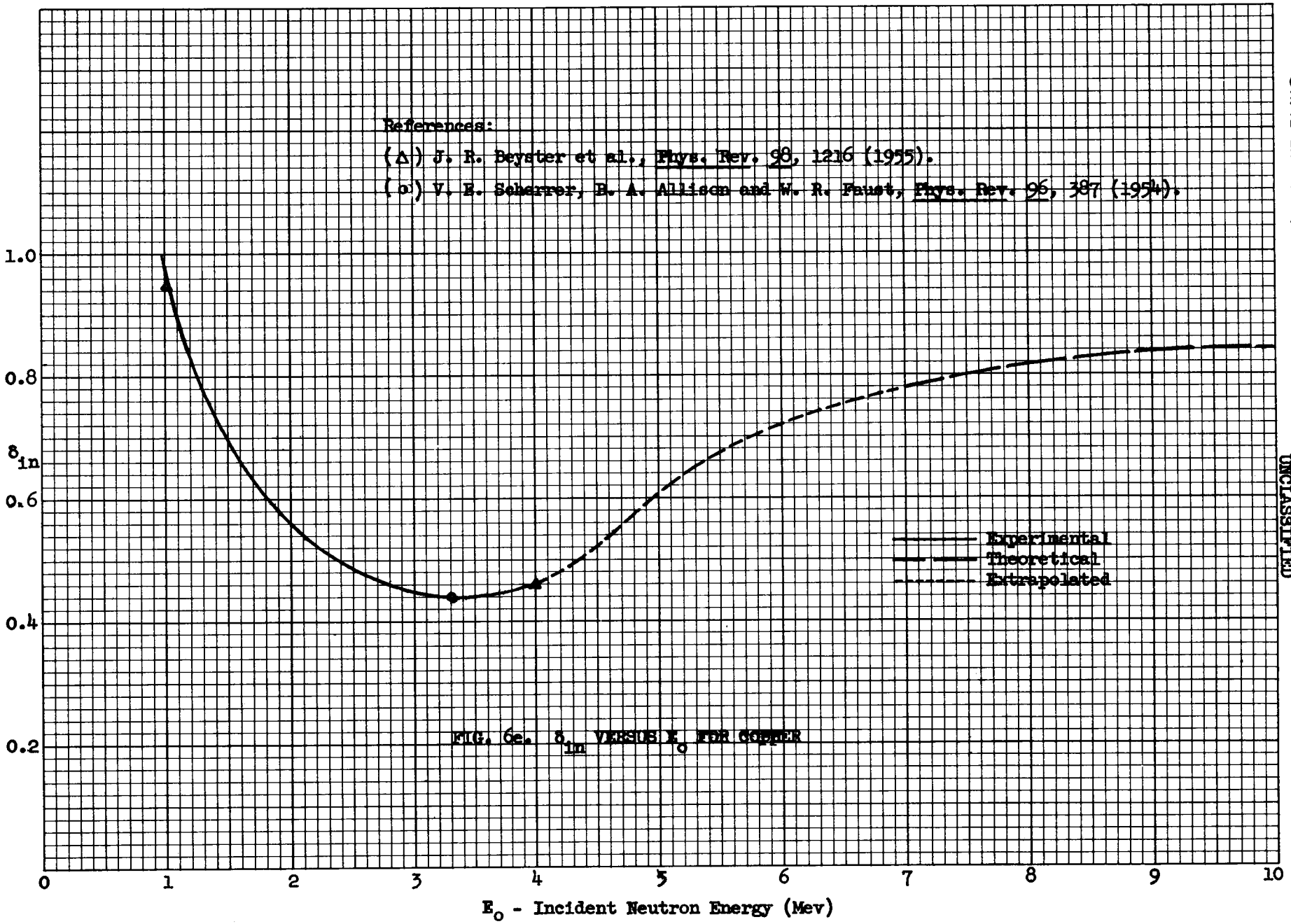

FIG. 6e. δ_{in} VERSUS E_o FOR COPPER

[redacted]

is approximately 0.5 Mev at E_o = 3 Mev,[34] while at 14 Mev, T of tungsten is approximately 0.61 Mev,[32] which results in a δ_{in} that is 8% higher for the energy dependent T at E_o = 3 Mev.

An average δ_{in} for the fuel, $\overline{\delta_{in}}$, was obtained by weighting the δ_{in}'s of the fuel constituents by their respective inelastic cross sections. A similar procedure was followed for the Inconel. The $\overline{\delta_{in}}$'s for the fuel and the Inconel can then be used directly with the respective macroscopic cross sections when estimating the inelastic gamma-ray source strengths in various fuel and Inconel regions.

The gamma-ray spectra from the interaction of 14-Mev neutrons with a number of elements have been obtained.[36] For the elements used the absorption and (n,2n) cross sections are small relative to the inelastic cross section. Thus the gamma-ray spectra obtained should be reasonably representative of those from the inelastic scattering of 14-Mev neutrons. The average photon energy increased with atomic number from 1.1 Mev for A = 12 to 1.6 for A = 60 and then decreased with increasing A to 0.8 Mev for A = 208. This agrees with another observation[27,37] that the relative number of observed gamma rays with energies greater than 3-Mev increases with atomic number up to A = 60 and then decreases. This can be explained by the fact that (n,2n) reactions have higher cross sections for heavier elements and comprise a greater portion of non-elastic cross sections than for the intermediate elements. Since the computed heat generation rates are relatively insensitive to the average photon energy used, the gamma rays from inelastic scattering are assumed to have an energy of 1 Mev in the heating calculations.

Table 10 gives the average value of $\Delta u\ \delta_{in}\ E_o\ \Sigma_{in}$ in several lethargy groups for the materials which it is believed will give contributions to the gamma-ray heating of the ART due to gamma rays from inelastically scattered

36. V. E. Scherrer, R. B. Theus and W. R. Faust, Phys. Rev. 91, 1476 (1953).
37. H. L. Taylor, O. Lönsjö and T. W. Bonner, Phys. Rev. 100, 174 (1955).

[redacted]

[redacted]

neutrons. In Table 10, $\Delta u \equiv$ width of the lethargy interval, and, given the flux, ϕ_i, in lethargy group i, the product

$\Delta u_i \left(\overline{\delta_{in} E_o \Sigma_{in}} \right)_i \phi_i$ = total gamma ray energy/sec·cm^3 originating at a given point due to neutrons in the i^{th} lethargy group at that point

= number of 1-Mev gamma rays/sec·cm^3 originating at a given point due to neutrons in the i^{th} lethargy group at that point.

[redacted]

[redacted]

Table 10. Values of $\Delta u \times \overline{\delta_{in} E_o \Sigma_{in}}$

Lethargy Group	Δu	$\Delta u \times \overline{\delta_{in} E_o \Sigma_{in}}$ for			
		Na	Cu	Inconel	Fuel
1	0.5	0.05432	0.4379	0.4200	0.1827
2	0.5	0.02886	0.1942	0.1928	0.09277
3	0.5	0.01506	0.06588	0.08757	0.03605
4	0.5	0.007771	0.02677	0.04169	0.01517
5	0.5	0.004535	0.007741	0.002091	0.007386
6	0.5	0.001832	0	0	0.005005
7	0.5	0			0.009030
8	0.5				0.009422
9	3.0				0.006157
10	3.0				0

[redacted]

[redacted]

BUILDUP FACTORS

The basic approach to the calculation of gamma-ray energy absorption that has been adopted in this work is to assume straight exponential absorption of the gamma rays, with narrow beam absorption coefficients, and to multiply the results so obtained by a buildup factor to account for the accumulation of lower energy gamma rays in the beam due to compton scattering (but not those due to bremsstrahlung and annihilation radiation, which are considered to be of very minor importance in the photon energy range of interest here).[38]

The energy absorption buildup factor for the materials in the ART is represented by the expression

$$B_a = A(e^{\alpha\mu r} - 1) + 1 ,$$

where μr is the number of mean free paths. This approximation for the buildup factor is a simplification of the double-exponential form suggested by Taylor[39] and seems to be quite adequate for distances less than 5 mean free paths. The values of A and α were found from the data given by Goldstein and Wilkins[38] in the following manner.

For compound materials (i.e., those consisting of more than one element) an equivalent atomic number Z was found by comparing the energy dependence of the gamma-ray absorption coefficients calculated for the mixture with that for pure materials. The data for this was taken from work by Moteff.[40] Since the gamma-ray absorption coefficient at any one particular energy is a slowly varying function of the atomic number, the equivalent Z can be determined to within ± 3. This is not a serious error for the intermediate and high Z materials, since in these ranges the variation of the buildup factor with atomic number is small. This could lead to serious errors in

---

38. H. Goldstein and J. F. Wilkins, Jr., Calculation of the Penetration of Gamma Rays, NYO-3075 (1954).
39. J. J. Taylor, Application of Gamma Ray Buildup Data to Shield Design, WAPD-Memo RM-217 (Jan. 25, 1954).
40. J. Moteff, Miscellaneous Data for Shielding Calculations, APEX-176 (1954).

[redacted]

[redacted]

the buildup factor for compound materials with a small equivalent Z. However, since the equivalent Z of water has been determined quite accurately by Goldstein and Wilkins and sodium (Z = 11) and Be (Z = 4) are not compound materials, the only bothersome material in this study is the B_4C. However this is composed of two elements whose atomic numbers differ only by one, and therefore the error in the equivalent Z must be less than ± 0.5. Thus, for all the compound materials dealt with here, there is very little error introduced into the buildup factors by the choice of the equivalent atomic numbers.

From the data of Goldstein and Wilkins,[38] plots were made of the energy absorption buildup factor for a point isotropic source as a function of the atomic number Z for several energies and three different values of gamma ray path length (1, 2, and 4 mean free paths). From these graphs the buildup factor for any Z can be found at any one of several energies and path lengths. By using the equivalent atomic number for compound materials, it is possible to plot the energy absorption buildup factor as a function of path length for a particular Z and a particular energy. A two-point fit to this curve was used to obtain the constants A and α in the equation given above. This is adequate for the present purpose, since in the gamma-ray energy deposition calculations short path lengths are, in general, of greatest importance.

The values of A and α given in Table 11 yield values of the buildup factor which vary less than 5% from the graphical values for distances less than 5 mean free paths.

Values of the equivalent Z, A and α are given for the following materials:

Fuel (5 mole % UF_4, 52.5 mole % NaF, 42.5 mole % ZrF_4)

Inconel (75 wt % Ni, 16 wt % Cr, 9 wt % Fe)[41]

NaK (56 wt % Na, 44 wt % K)[42]

---

41. T. J. Balles, ART Design Data Sheet No. 10-B-1 (Aug. 12, 1955).
42. T. J. Balles, ART Design Data Sheet No. 10-E-2 (Mar. 6, 1955).

[redacted]

[redacted]

Table 11. Formula for Energy Absorption Buildup Factor

$$B = A(e^{\alpha \mu_T r} - 1) + 1^*$$

Material	Z		Energy (Mev)						
			0.5	1	2	4	6	8	10
Be	4	A	2.66	4.16	7.33	59.0	-24.5	18.6	-6.73
		α	0.46	0.25	0.11	0.01	-0.02	0.02	-0.05
Na	11	A	4.52	4.98	8.03	56.4	41.2	21.0	-26.8
		α	0.31	0.21	0.10	0.01	0.01	0.015	-0.01
NaK	13	A	5.69	6.57	6.70	21.4	53.5	-12.7	50.5
		α	0.26	0.17	0.115	0.025	0.0075	-0.025	0.005
Inconel	27	A	12.8	7.18	8.08	6.19	3.14	1.99	1.25
		α	0.13	0.15	0.09	0.07	0.09	0.10	0.12
Heat Exchanger	32	A	17.8	8.78	8.08	5.43	2.00	1.48	1.22
		α	0.09	0.125	0.09	0.075	0.125	0.12	0.12
Fuel	48	A	-50.8	43.8	7.85	2.19	1.31	1.025	0.616
		α	-0.025	0.025	0.09	0.15	0.15	0.14	0.17
Boron Carbide	5.5	A	2.77	4.64	7.24	58.7	-47.0	-10.1	-6.51
		α	0.44	0.23	0.11	0.01	-0.01	-0.04	-0.05
H_2O	7.5	A	3.39	5.03	8.13	38.5	87.2	-9.60	-4.93
		α	0.385	0.215	0.10	0.015	0.005	-0.040	-0.065

* This formula is good up to about five relaxation lengths.

[redacted]

[redacted]

Heat exchanger (33.5 vol % fuel, 40.8 vol % NaK, 25.6 vol % Inconel)[43]

Boron Carbide (35 wt % C, 65 wt % B)[44]

Sodium

Beryllium

Water

LINEAR GAMMA-RAY ABSORPTION COEFFICIENTS

The linear total and energy absorption coefficients for gamma rays are given in both tabular and graphical form as a function of energy (Tables 12 and Figs. 7a through 7h). Values are given for all the materials comprising the ART. They were calculated from the μ/ρ values given by Moteff.[40]

For compound materials such as fuel, the density of each element in the compound was calculated first. Then $\mu(cm^{-1})$ was calculated from the μ/ρ values for this element at various energies. The μ for the compound at each energy was then obtained by adding the μ's of each element at the energy. The densities were determined at the operating temperature of the ART for all materials except Inconel. The μ/ρ values for nickel and iron were used for those of Inconel and stainless steel, respectively.

---

43. Calculated from data in ART Design Memo No. 8-J-3, Rev. 1 (Dec. 2, 1955).
44. Calculated from Specification No. JS-P3-22.

[redacted]

[redacted]

Table 12. Linear Gamma-Ray Absorption Cross Sections for the ART

Energy	Cross Sections (cm^{-1})							
	Fuel	Heat Exchanger	Boron Carbide Layer	Inconel	Na	Be	Cu	Stainless Steel
	Total Absorption Cross Sections, μ_T							
0.5	0.304	0.308	0.169	0.695	0.064	0.134	0.713	0.618
1.0	0.198	0.215	0.128	0.512	0.047	0.095	0.496	0.443
2.0	0.136	0.150	0.085	0.360	0.033	0.068	0.359	0.322
3.0	0.117	0.128	0.068	0.305	0.027	0.053	0.309	0.273
4.0	0.107	0.117	0.058	0.280	0.023	0.045	0.283	0.249
5.0	0.101	0.111	0.052	0.271	0.021	0.040	0.272	0.238
6.0	0.099	0.110	0.047	0.267	0.020	0.036	0.266	0.230
8.0	0.095	0.109	0.041	0.267	0.018	0.030	0.267	0.225
10.0	0.095	0.106	0.037	0.263	0.017	0.027	0.270	0.227
	Energy Absorption Cross Sections, μ_E							
0.5	0.133	0.121	0.057	0.267	0.023	0.044	0.270	0.231
1.0	0.094	0.100	0.053	0.229	0.021	0.041	0.228	0.197
2.0	0.075	0.084	0.046	0.197	0.018	0.036	0.196	0.173
3.0	0.073	0.079	0.040	0.186	0.016	0.031	0.191	0.168
4.0	0.073	0.080	0.037	0.190	0.015	0.028	0.196	0.168
5.0	0.074	0.081	0.034	0.196	0.014	0.026	0.200	0.171
6.0	0.075	0.085	0.031	0.212	0.014	0.024	0.209	0.174
8.0	0.078	0.088	0.029	0.222	0.013	0.021	0.219	0.183
10.0	0.080	0.090	0.027	0.225	0.013	0.020	0.233	0.192

[redacted]

[redacted]

FUEL

Fig. 7a
Linear Absorption Coefficient
vs
Energy for the Fuel

NaF	52.5 mole %
ZrF_4	42.5 mole %
UF_4	5.0 mole %

ρ = 3.2 gm/cm^3 at ~ 1400°F

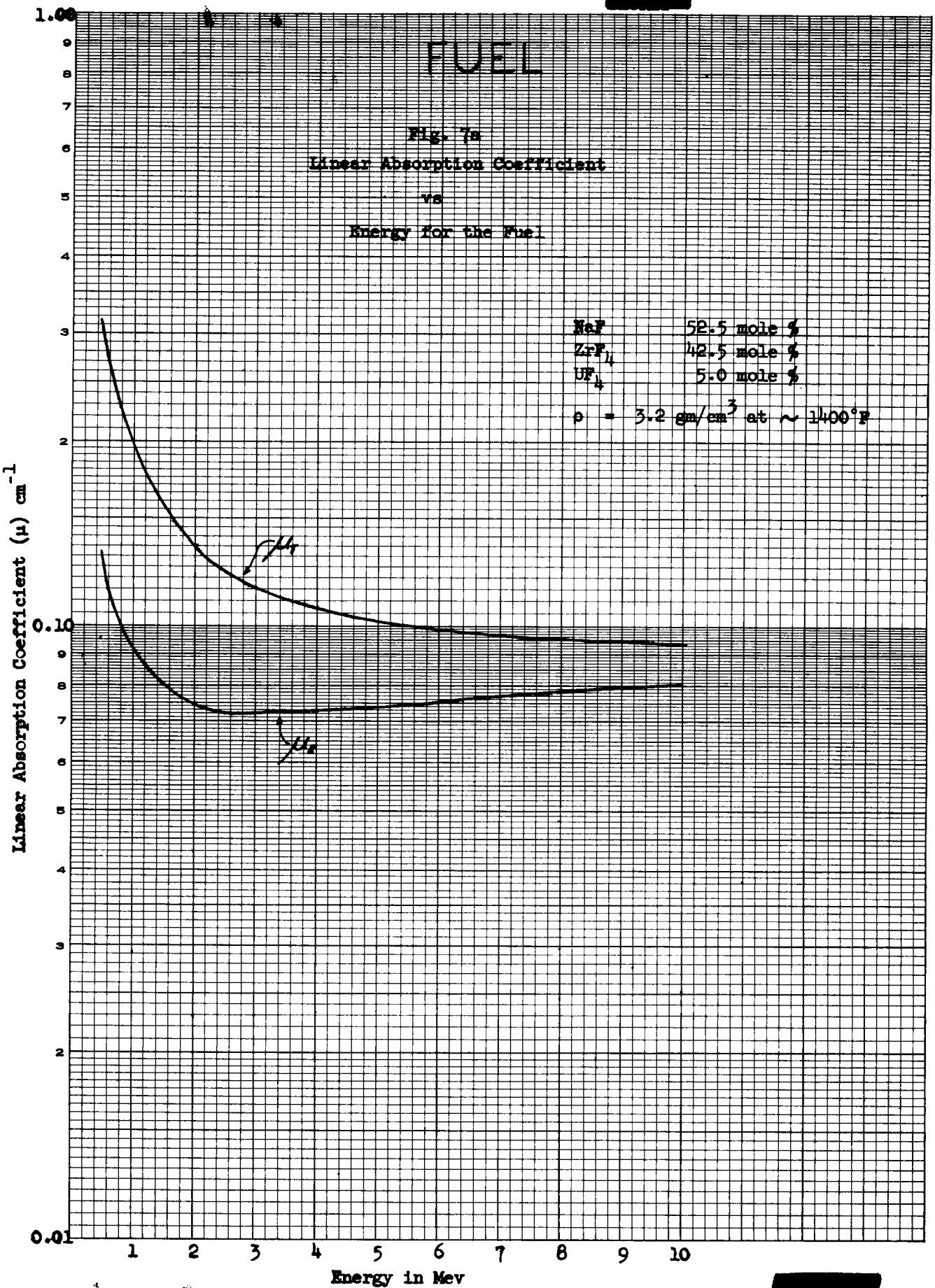

[redacted]

ORNL-LR-DWG. 14370

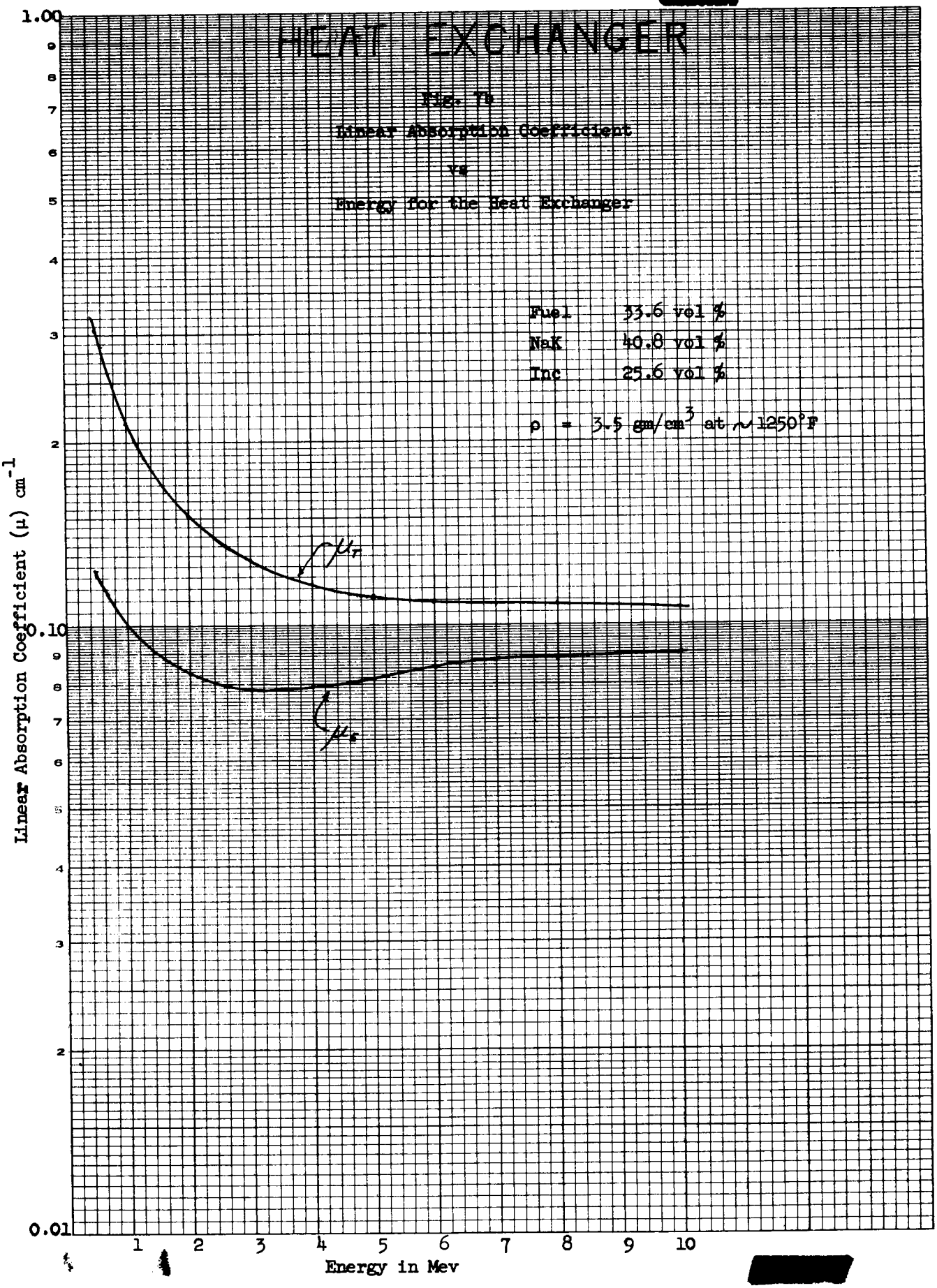

ORNL-LR-DWG. 14371

UNCLASSIFIED

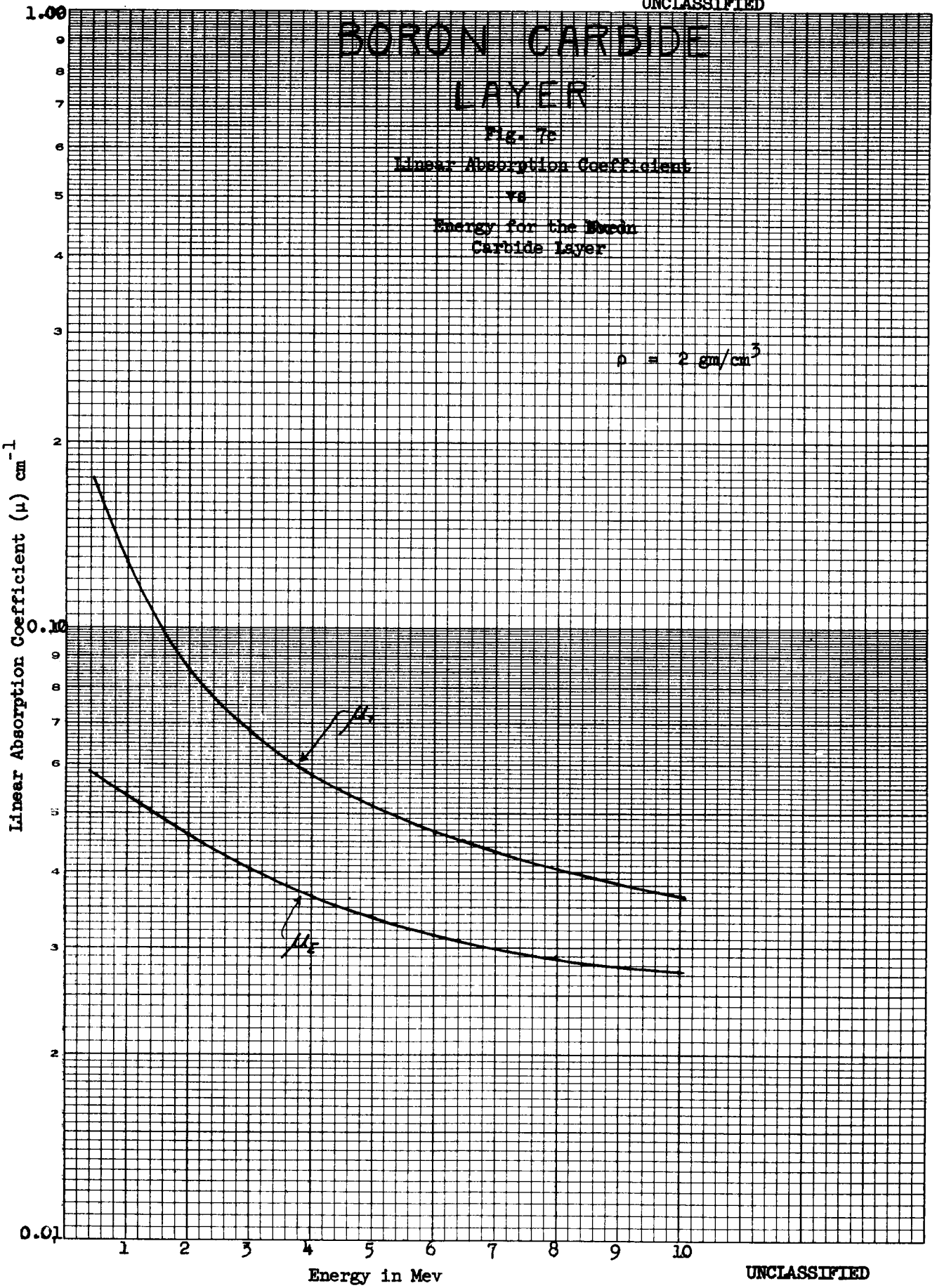

UNCLASSIFIED

ORNL-LR-DWG. 14372

UNCLASSIFIED

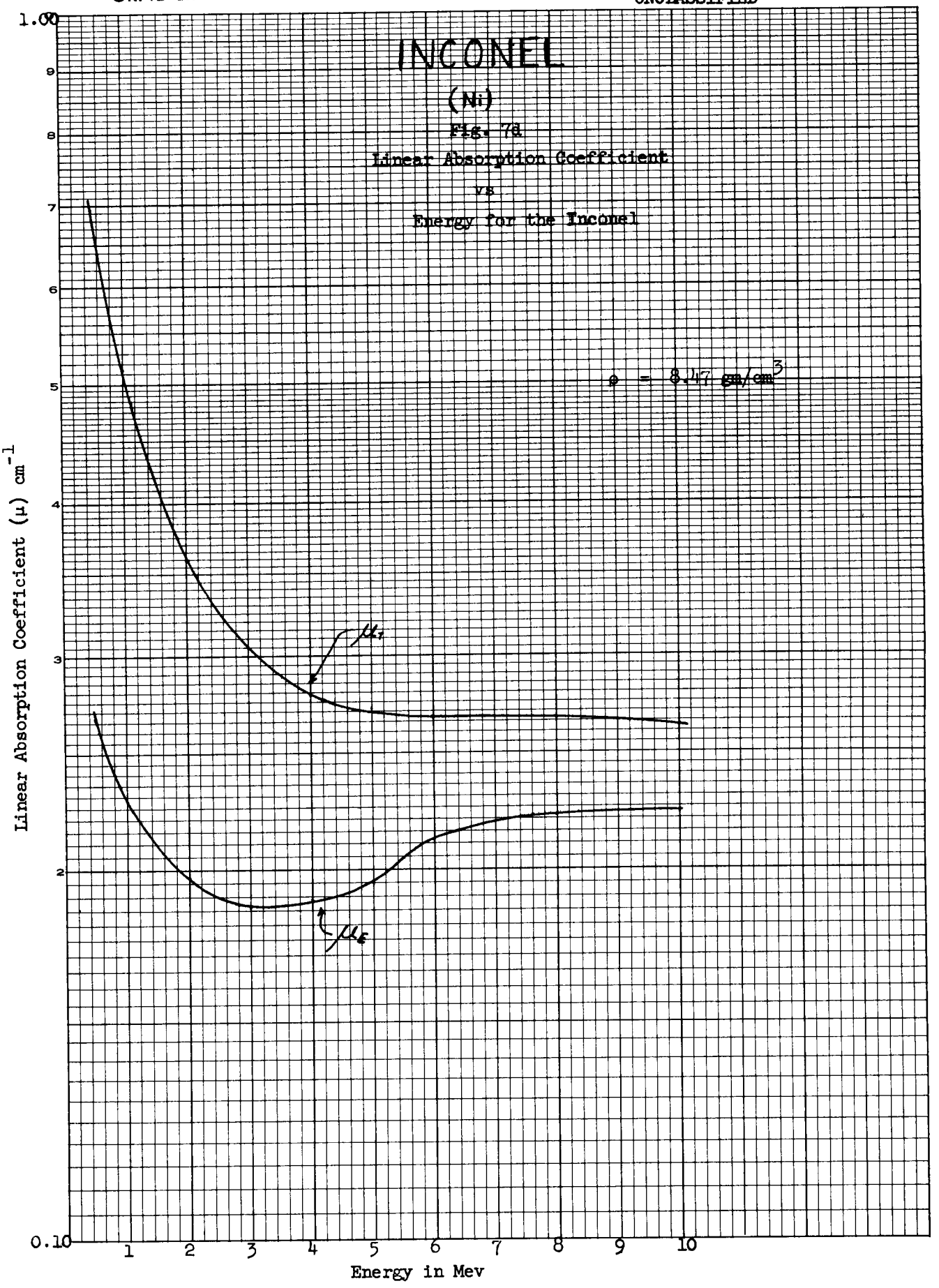

UNCLASSIFIED

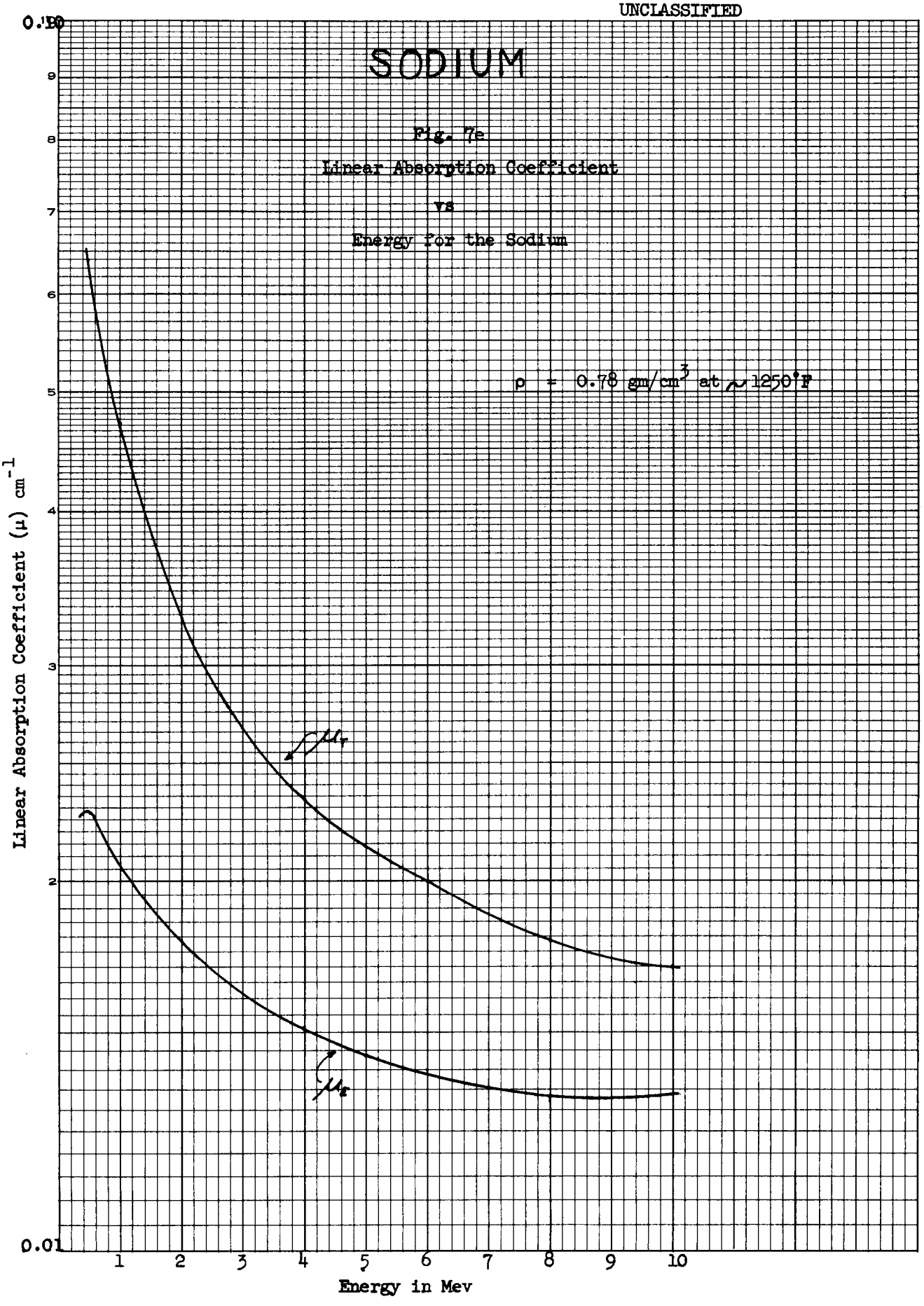

ORNL-LR-DWG. 14374

UNCLASSIFIED

BERYLLIUM

Fig. 71

Linear Absorption Coefficient

vs

Energy for the Beryllium

ρ = 1.69 gm/cm^3 at ~1250°F

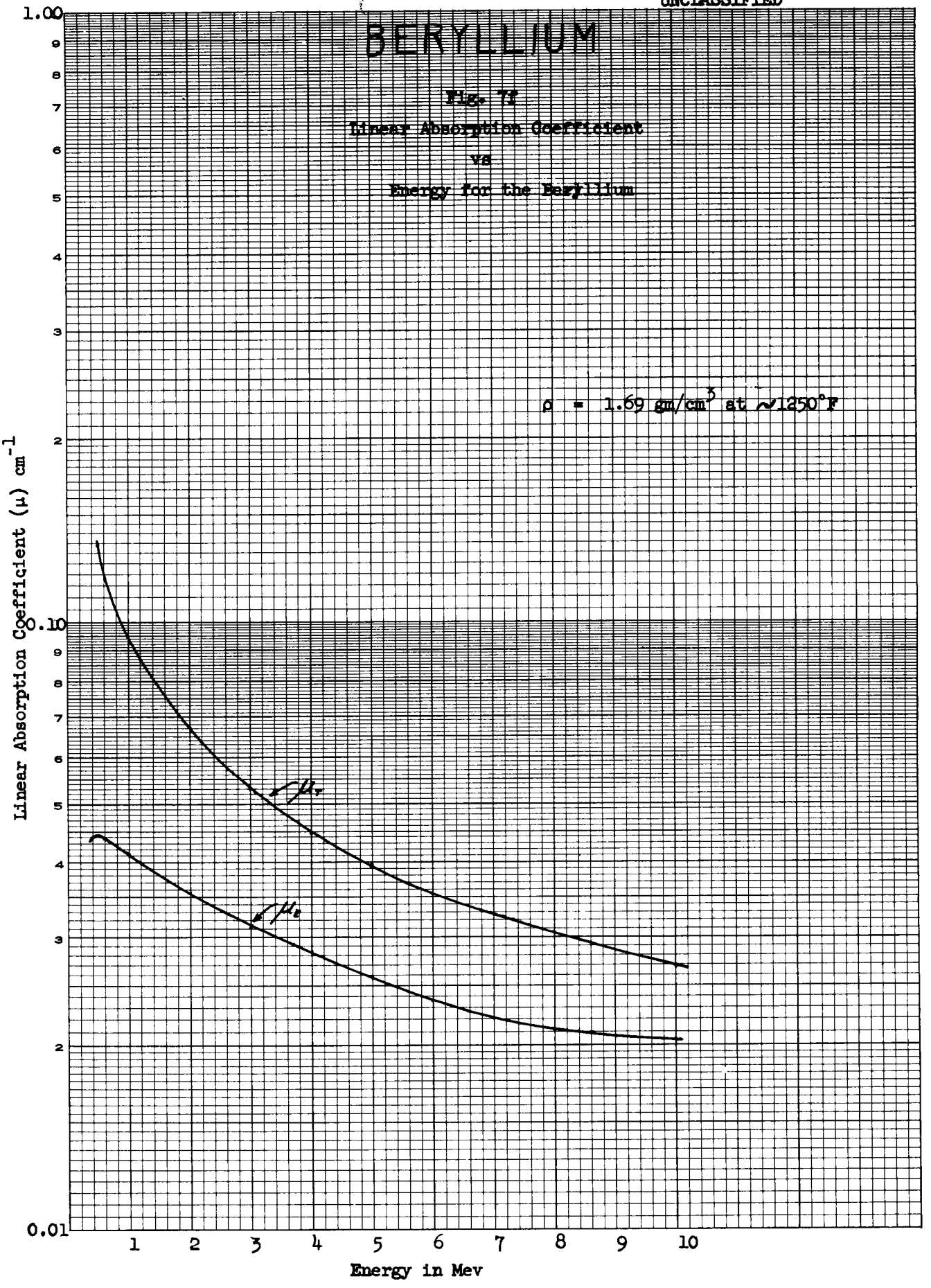

UNCLASSIFIED

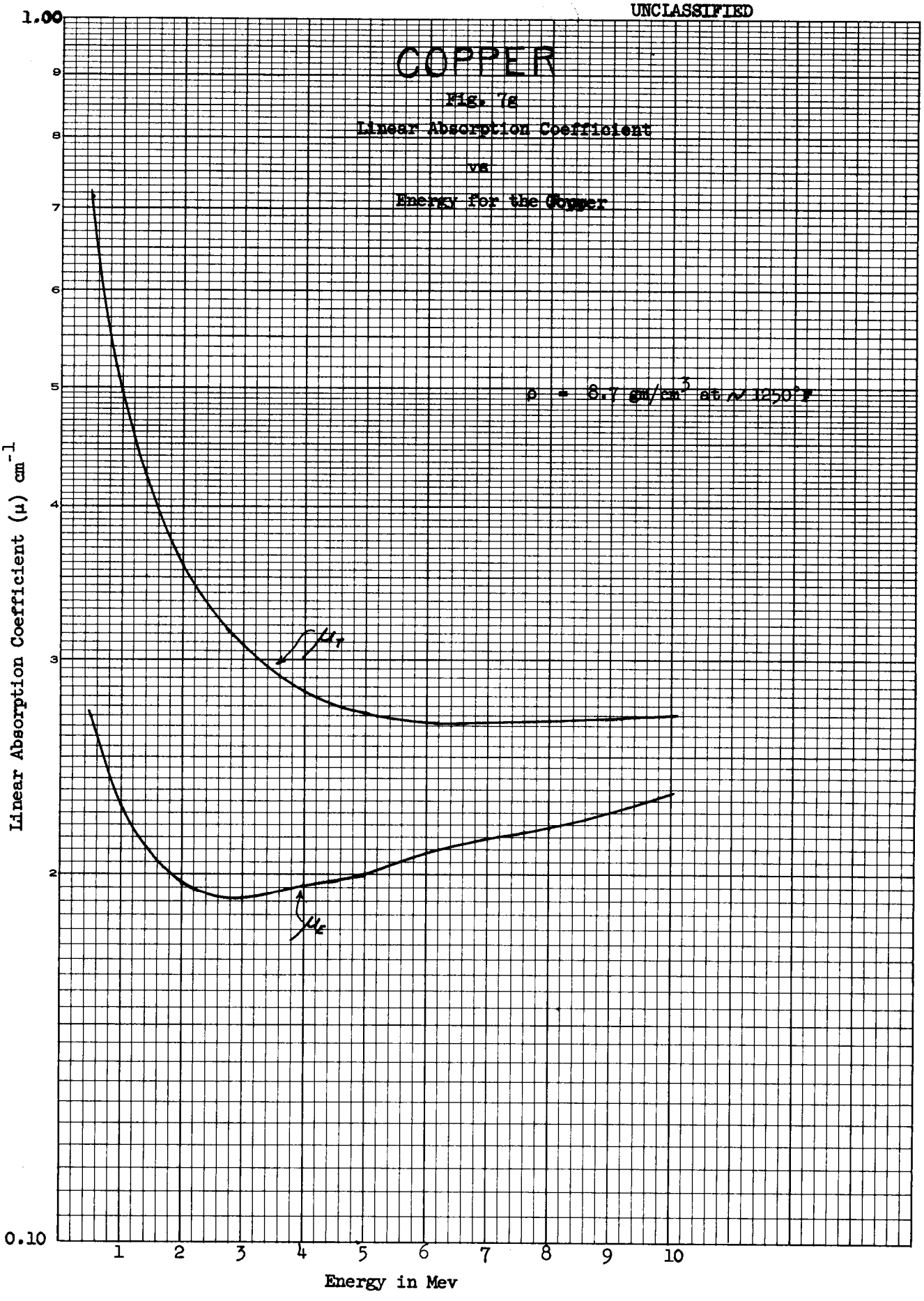

ORNL-LR-DWG. 14376 UNCLASSIFIED